

Large-Scale Air-Sea Interactions and Climate Variability: ENSO

Lecture - 11

B. N. Goswami

**SERB Distinguished Fellow
Cotton University, Guwahati**

4 June, 2022

Air-Sea Interactions

Small-scale air-sea Interactions

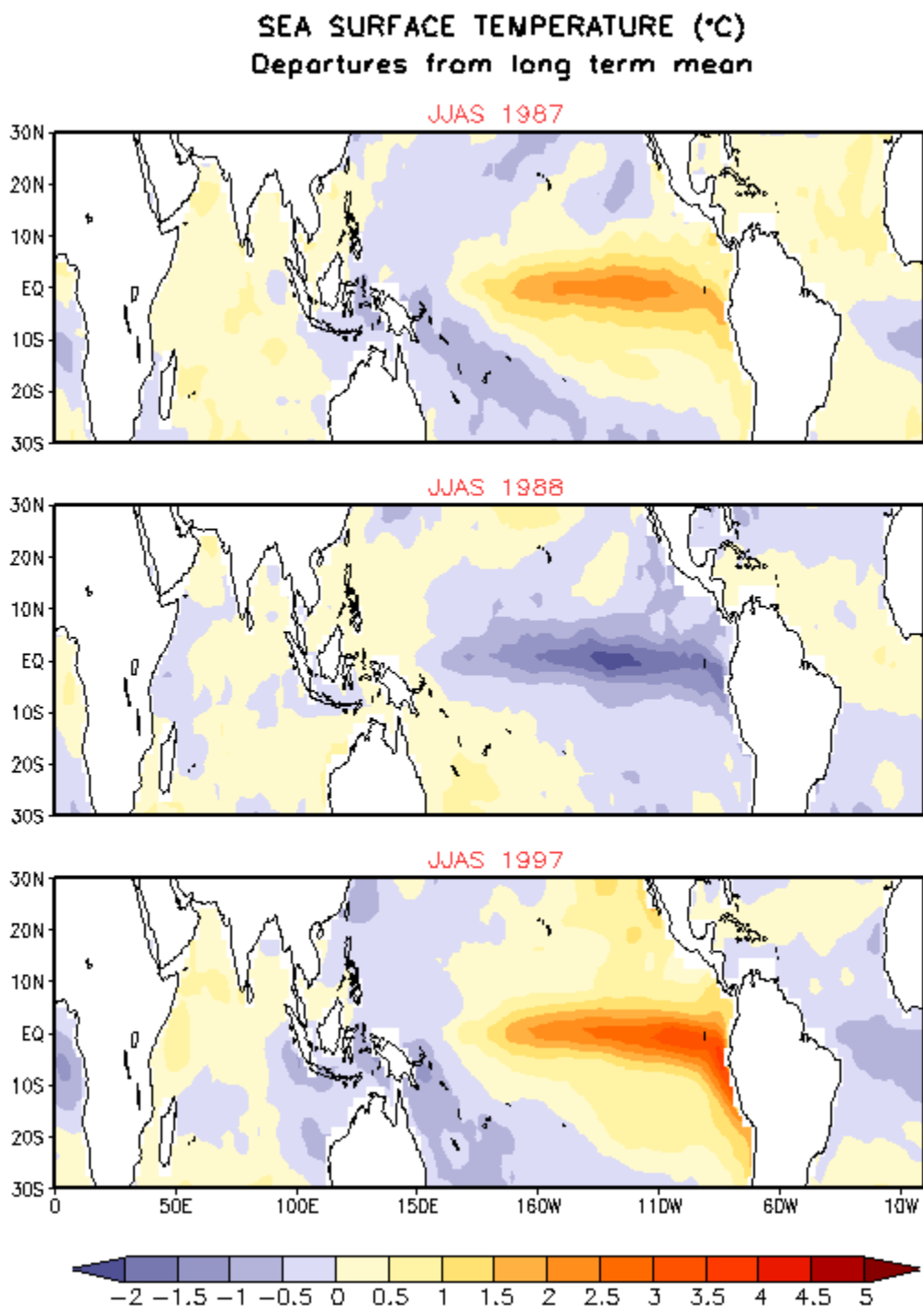
- Turbulence in the Ocean mixed layer help transmit atmospheric momentum (winds) to the Ocean leading to Ocean currents.
- Turbulence in the ABL help heat and water vapor fluxes from Ocean surface to be mixed to the cloud base leading to cloud formation and atmospheric heating.
- Such exchanges could lead to local air-sea interactions.
For Ex. $E \sim C_D \times V_s \times (q_s - q_a)$, $q_s = f(\text{sst})$, $q_a = f(T_a)$
- Atmospheric winds and SST both $\rightarrow E \rightarrow$ cools SST \rightarrow influences $E \rightarrow$ Conv. (q) in ABL above SST (e.g. by synoptic events) \rightarrow Clouds \rightarrow Atmos. heating \rightarrow change in $V_s \rightarrow$ change in E
- Basis for air-sea interaction on local scale

Air-Sea Interactions

Planetary scale air-sea Interactions

- Recall that the Solar radiation is the primary 'external' forcing for the mean Climate. Hence, major 'externally' forced climate variations are on Milankovitch time scales, 21K, 42K and 100K year time scales
- However, there are climate variability on much shorter time scales, such as the ENSO ($T \sim 4$ years), multi-decadal variability of ISMR ($T \sim 65$ years) etc
- These are 'internal' to the Climate System. Ocean, Atmosphere and Land interact on a planetary scale to produce these climate variability:

In this Lecture, I use El-Nino and Southern Oscillation (ENSO) as an example to illustrate how large-scale air-sea interactions can lead to inter-annual Climate Variability.

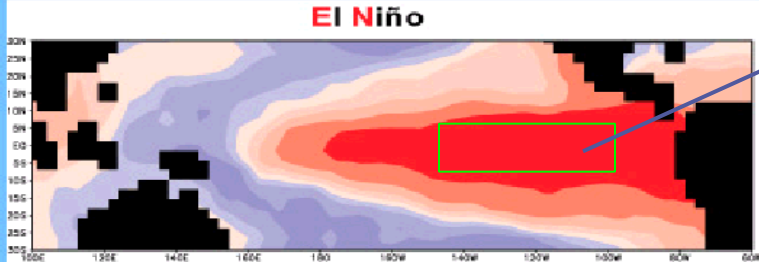


What is ENSO?

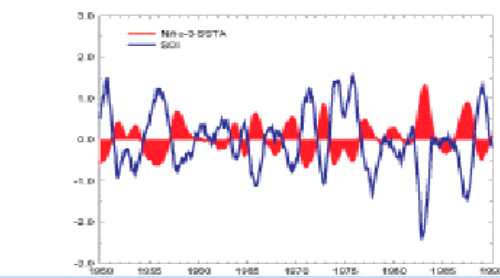
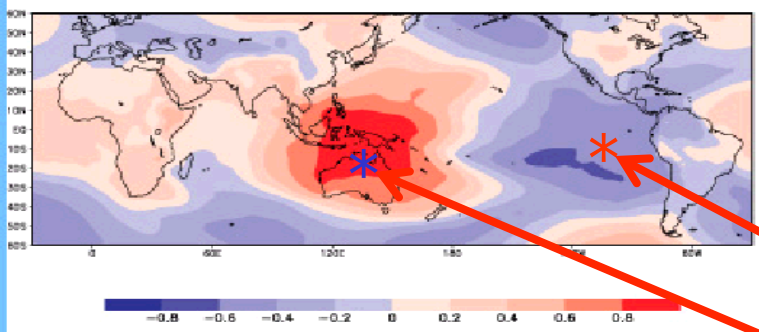
The equatorial central & eastern Pacific Ocean alternates between large scale warming (El Nino) and cooling (La Nina) at irregular intervals.

ENSO Fundamentals

El Niño



Southern Oscillation



Upper panel: A typical¹ anomaly pattern for the tropical Pacific sea surface temperature (SST) associated with El Niño. Shown is the correlation of annual SST anomalies averaged over the Niño-3 region (5°N - 5°S , 150°W - 90°W) with all other locations. Middle: Spatial structure of the Southern Oscillation showing the global-scale nature of the phenomenon. Shown is the correlation of annual pressure anomalies at Djakarta (Indonesia) with all other locations. Lower: Time series of the Southern Oscillation Index (SOI; blue line) which measures the atmospheric sea-level pressure gradient across the tropical Pacific basin and of the anomalous SST averaged over the central equatorial Pacific (red line). Both time series are normalised by their standard deviation (courtesy of M. Latif, S. Venzke).

Nino-3

Canonical SST pattern associated with El Nino

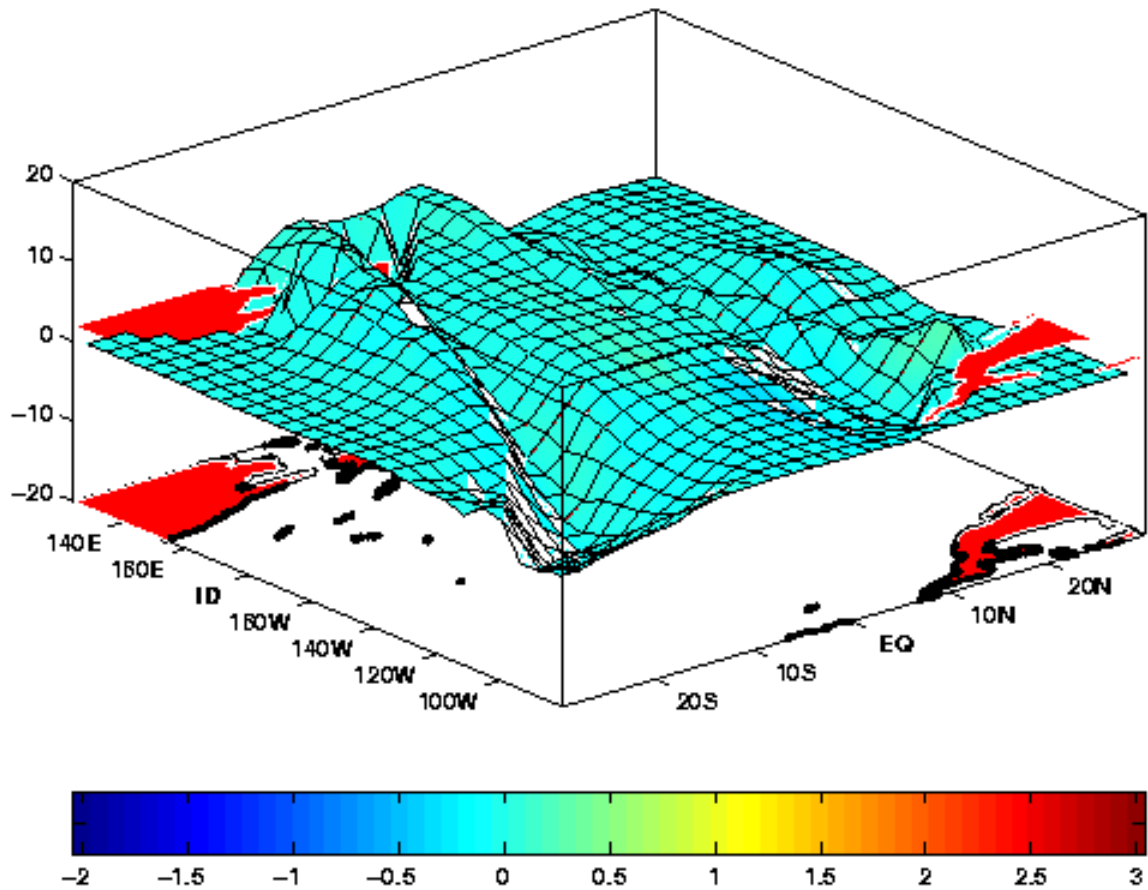
Sea-level pressure (SLP) variations associated with El Nino

Tahiti
Darwin

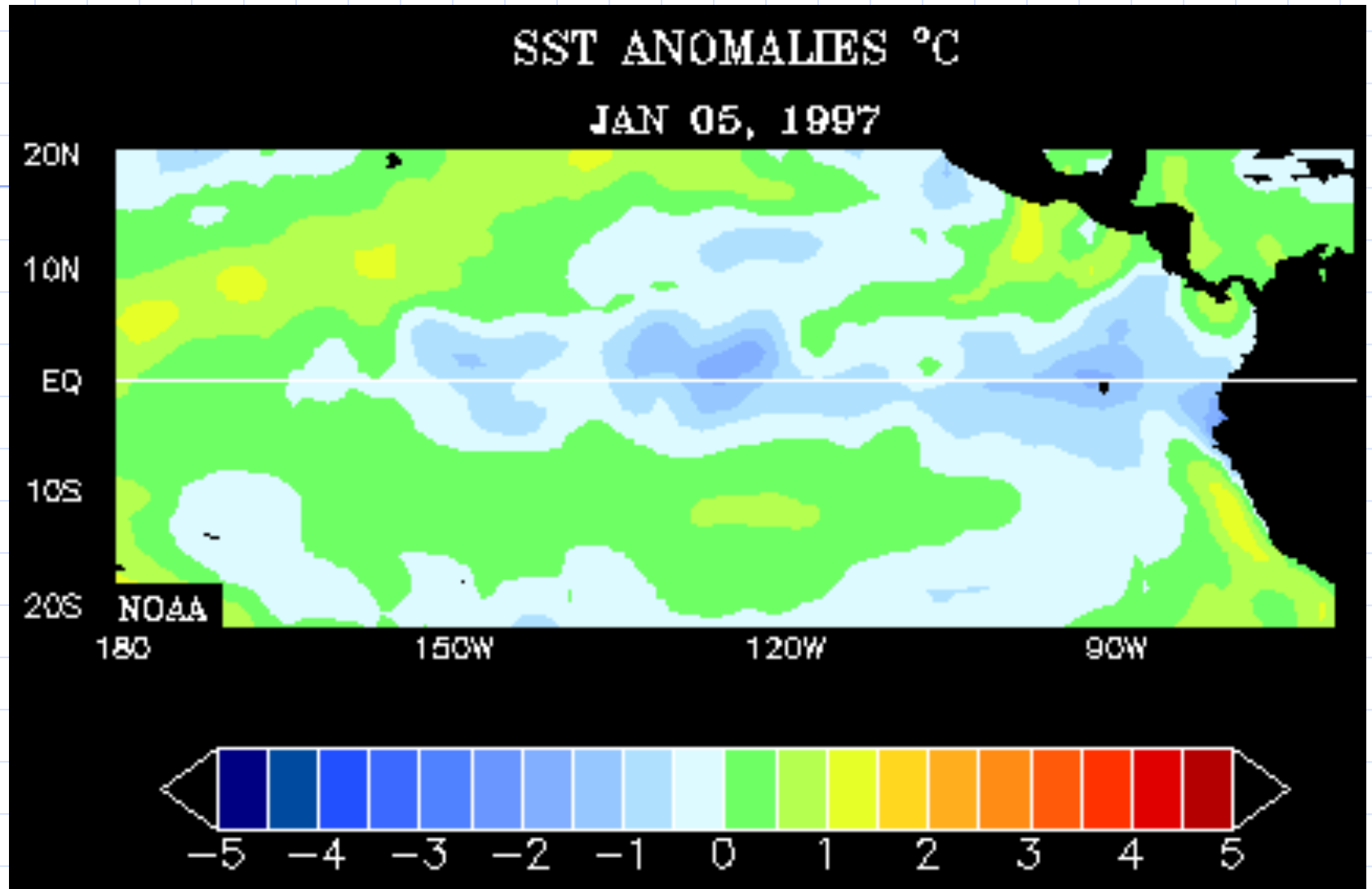
See-saw of SLP between eastern Pacific and Indonesia associated with El Nino is Southern Oscillation (SO)

SOI = Tahiti (SLP) – Darwin (SLP)

SEA LEVEL ANOMALY (surface, cm) and OCEAN TEMPERATURE ANOMALY (color, °C)

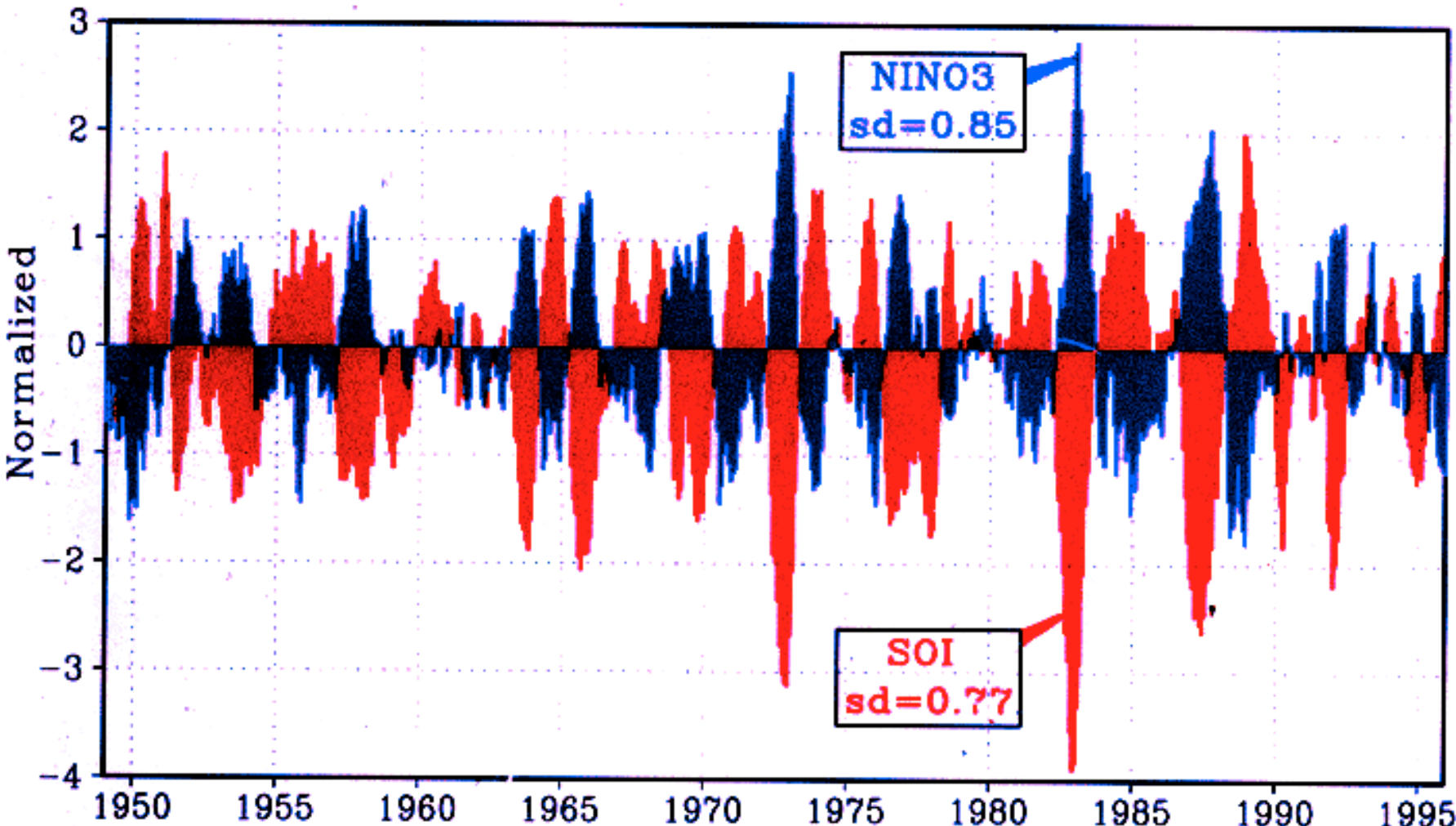


Evolution of sea level (contours) and sea surface temperature (color) across the tropical Pacific during ENSO cycle



Evolution of SST anomalies between Jan 1997 and Dec 1998

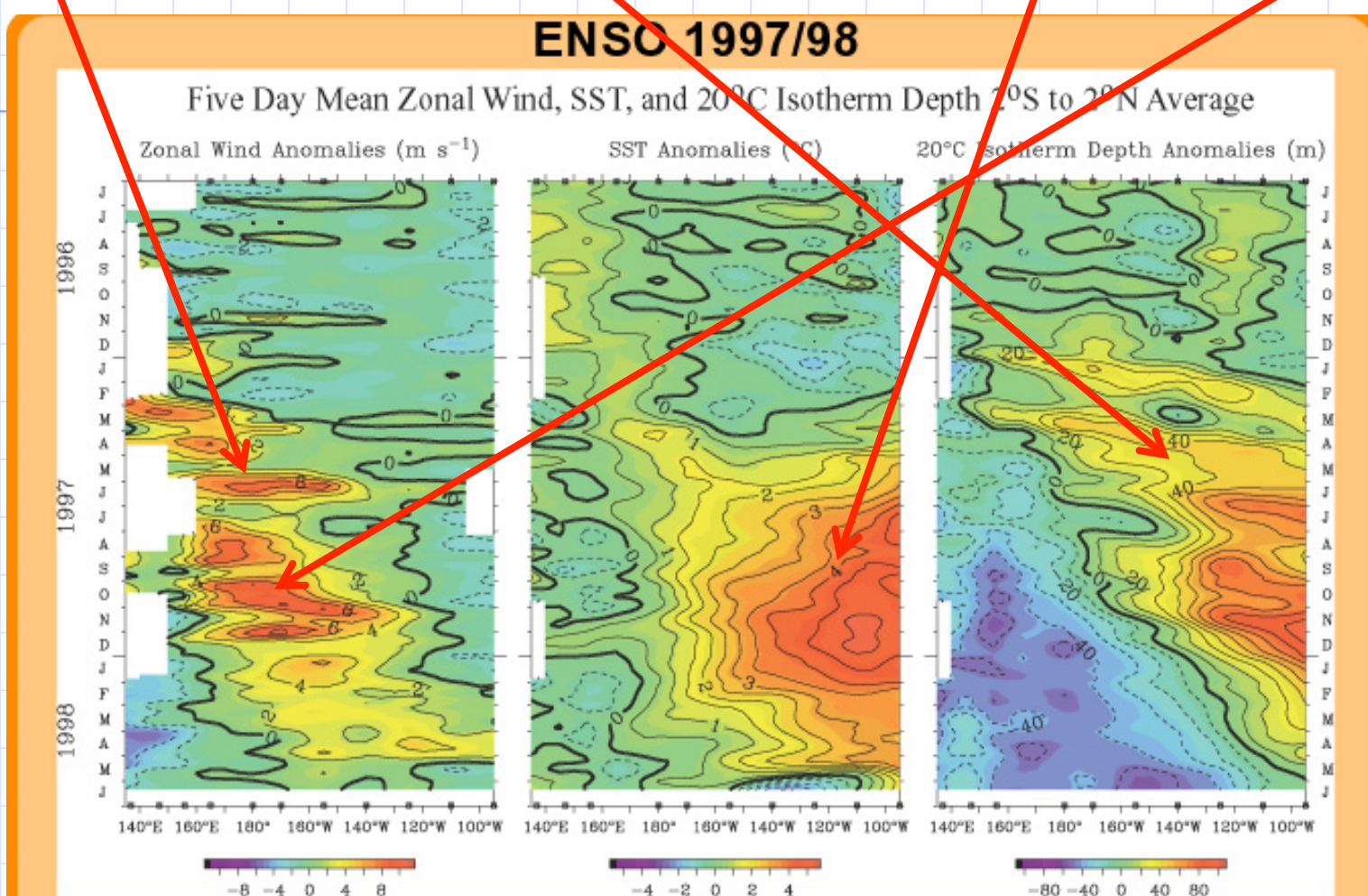
Indication of Ocean-Atmosphere Coupling.



Normalized time series of SST anomalies over Nino 3 area (blue) and Southern Oscillation Index (SOI, red). Strong correlation between the two is indicative of EN and SO being Ocean and Atmosphere components of the ENSO.

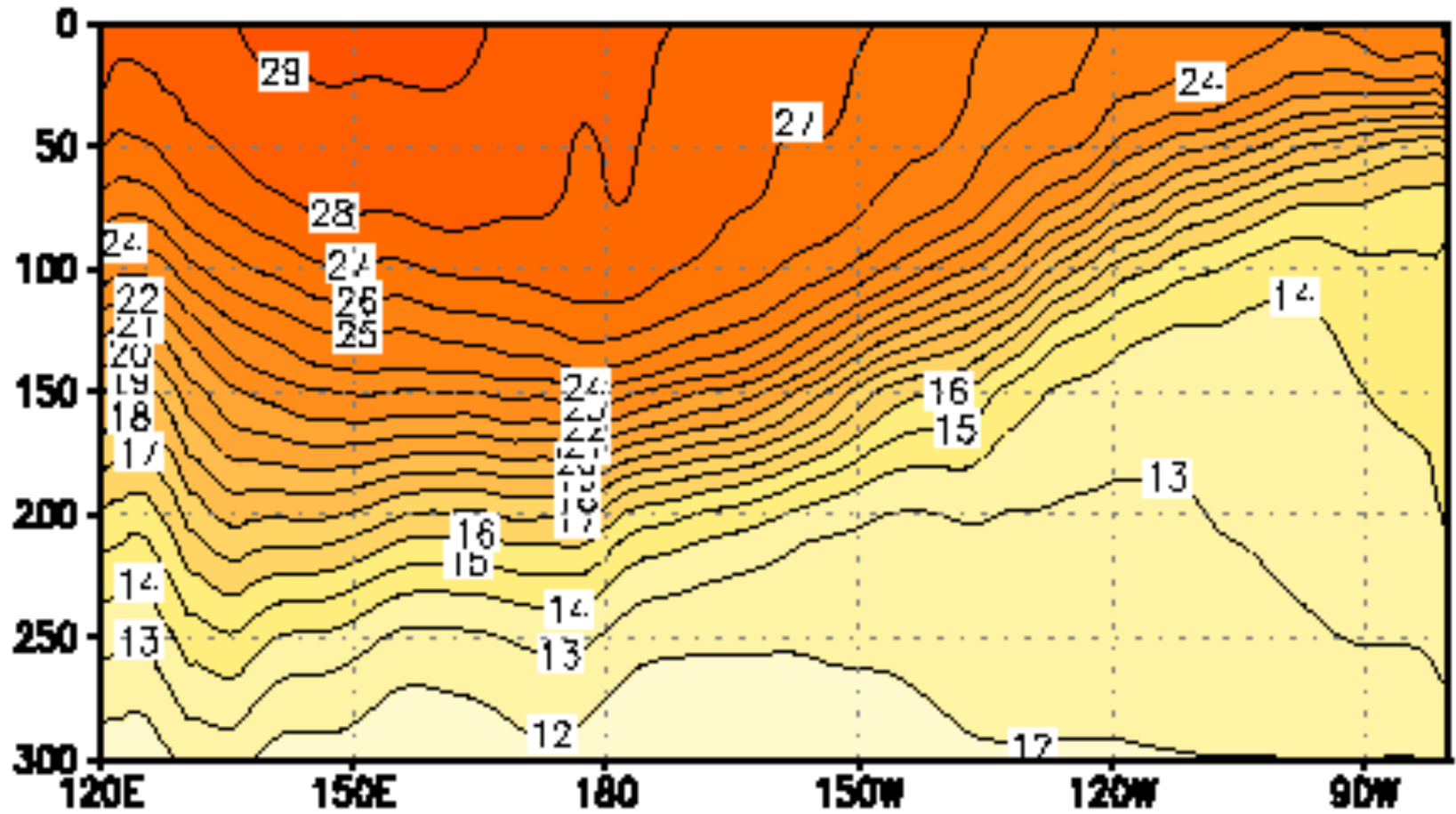
Further evidence of Ocean-Atmosphere Coupling

Westerly bursts → Ocean Kelvin waves → SST ↑ → Westerly ↑



Time / longitude sections of anomalies in the surface zonal winds (in m s^{-1}), SST (in $^{\circ}\text{C}$) and 20°C isotherm depth (in m) for the past 24 months. Analysis is based on 5-day averages between 2°N-2°S of moored time series from the TAO array. Anomalies are relative to monthly climatologies cubic spline fitted to 5-day intervals (COADS winds, Reynolds SST, CTD/XBT 20°C depths). Positive winds are westerly. Squares on the abscissas indicate longitudes where data were available at the start of the time series (top) and at the end of the time series (bottom). The TAO array is presently supported by the US (NOAA Office of Global Programs), Japan (JAMSTEC), Taiwan (NSC), Korea (STA) and France (ORSTOM). Further information is available from Dr. M.J. McPhaden (NOAA/PMEL) (courtesy of NOAA/PMEL).

Cross section of water temperature over equatorial Pacific as a function of depth showing the east-to-west sloping Thermocline. Also note the 20° isotherm indicating WWV

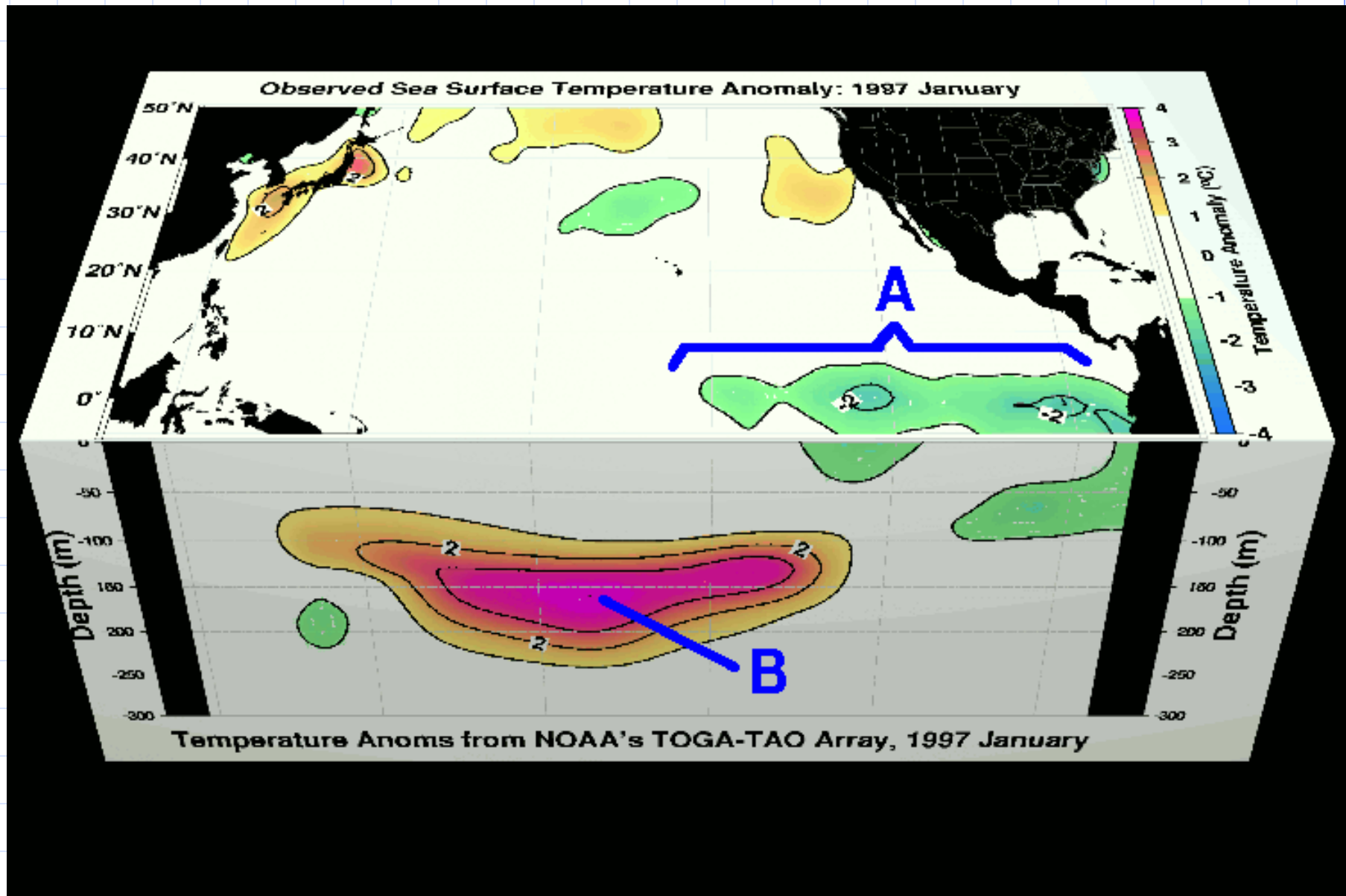


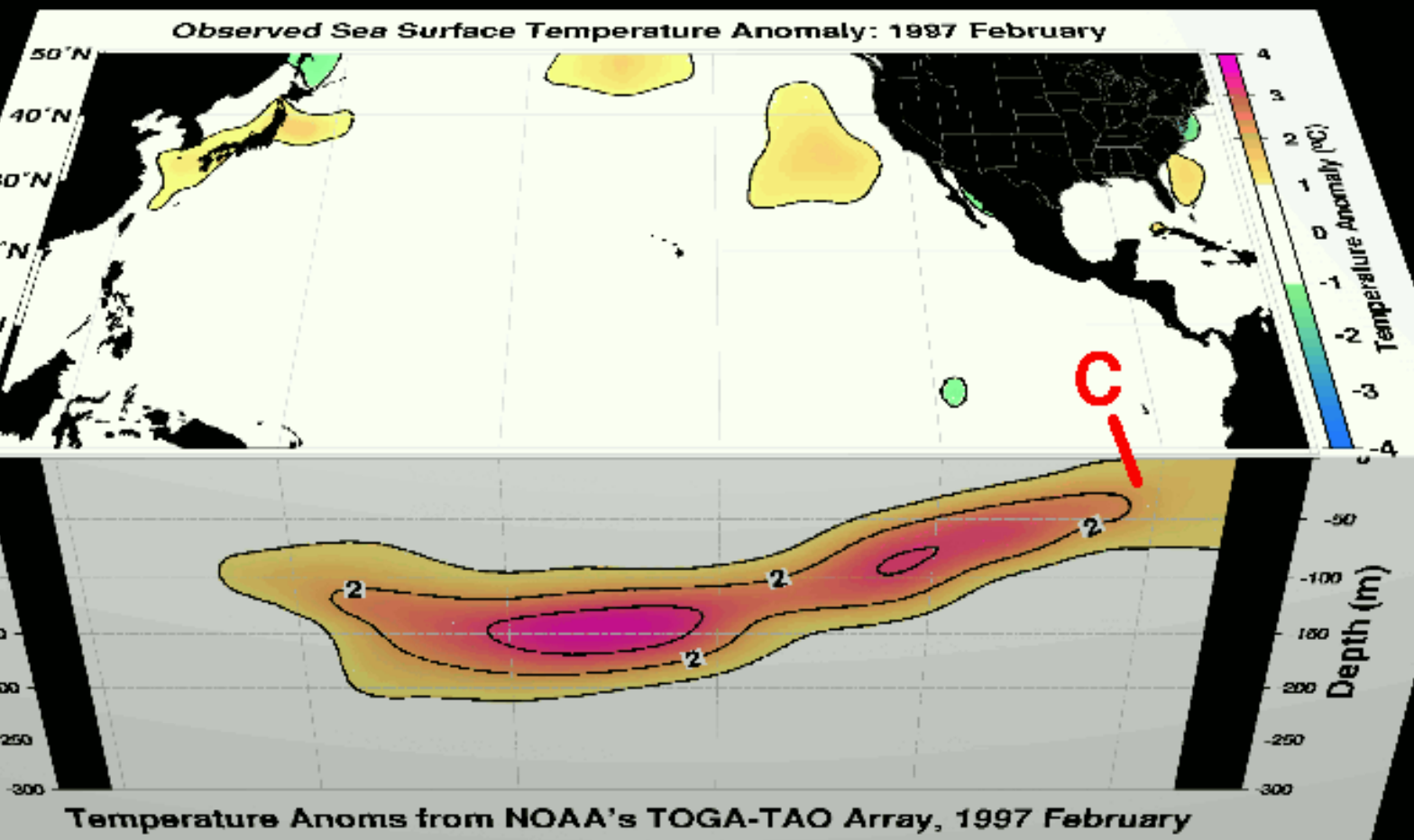
Water temperature with depth along the equatorial Pacific

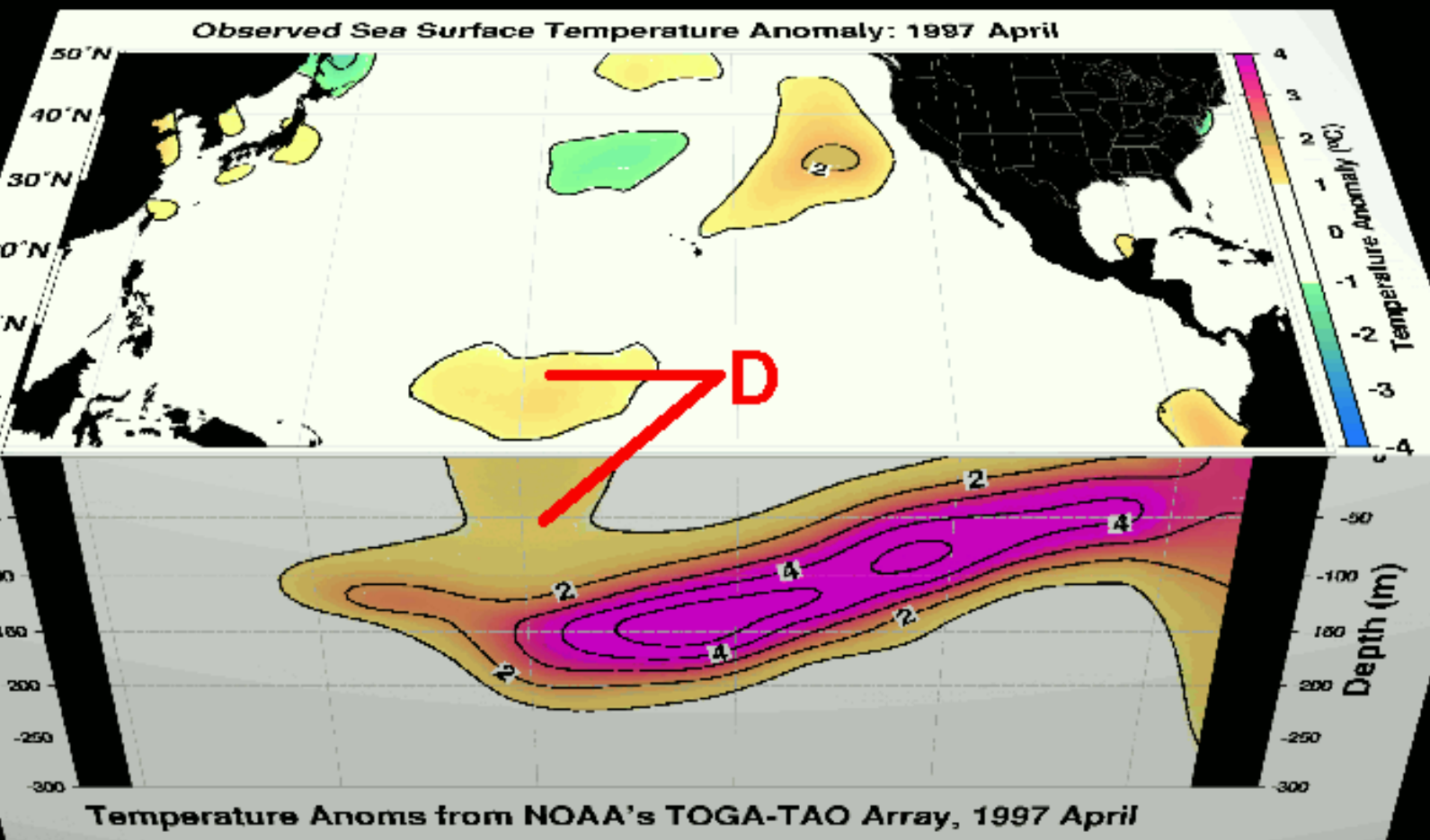
Next figure depicts a sequence of longitude-depth cross-sections of mean temperature in the equatorial Pacific Ocean for the months from January 1997 to May 1998. This period corresponds to the onset and intensification of the 1997-98 El Nino event. Clearly evident in Figure is the normal pooling of very warm water and the depression of the thermocline in the western Pacific in January 1997, and the eastward march of warmer than normal temperatures (positive temperature anomalies) from this region during the 1997-98 El Nino event. Notice the extensive cap of exceptionally warm surface waters in the eastern Pacific in January of 1998, the tell-tale signal of the arrival of El Nino in the Pacific coastal waters of equatorial South America. One can well imagine that the presence of this abnormally warm water profoundly influences and interferes with the normal upwelling of cold deep water and the delivery of life-sustaining nutrients to the base of the marine food chain.

It is interesting to note that a large pool of subsurface cold water formed in the western Pacific in January 1998, when the El Nino was in its peak in the eastern Pacific.

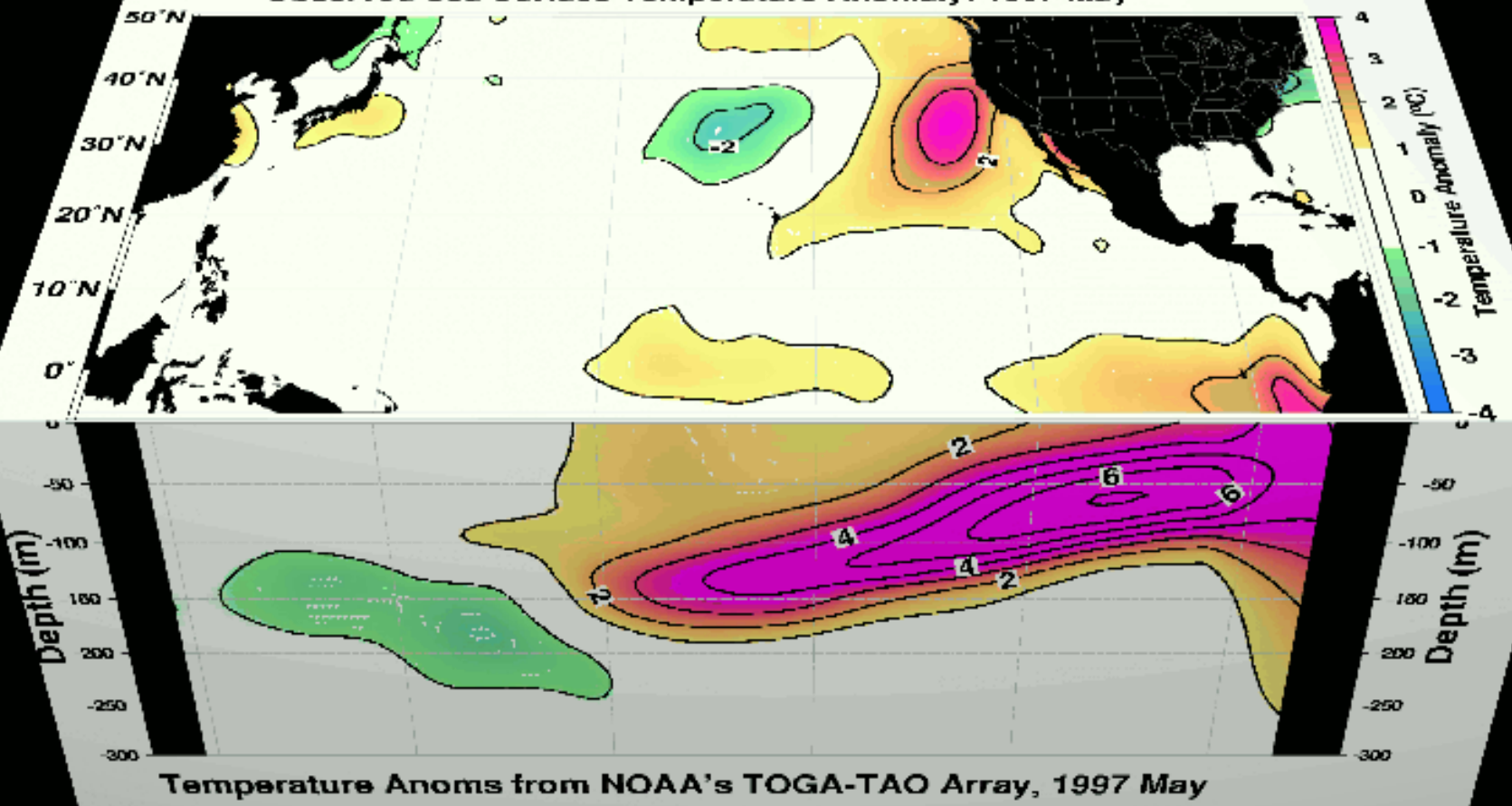
Evolution of sub-surface and surface temperature anomalies during 1997-98 super El Nino event.

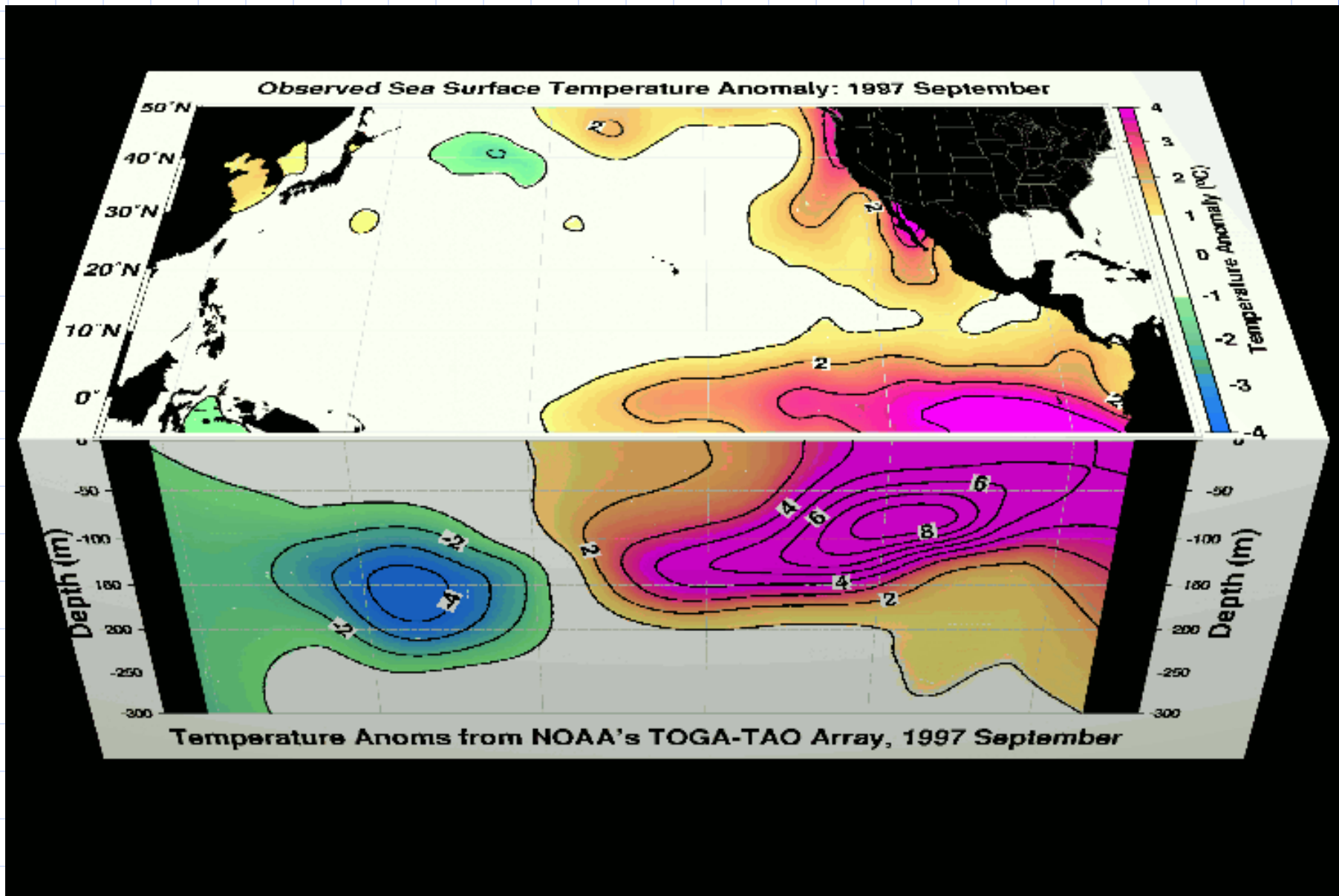


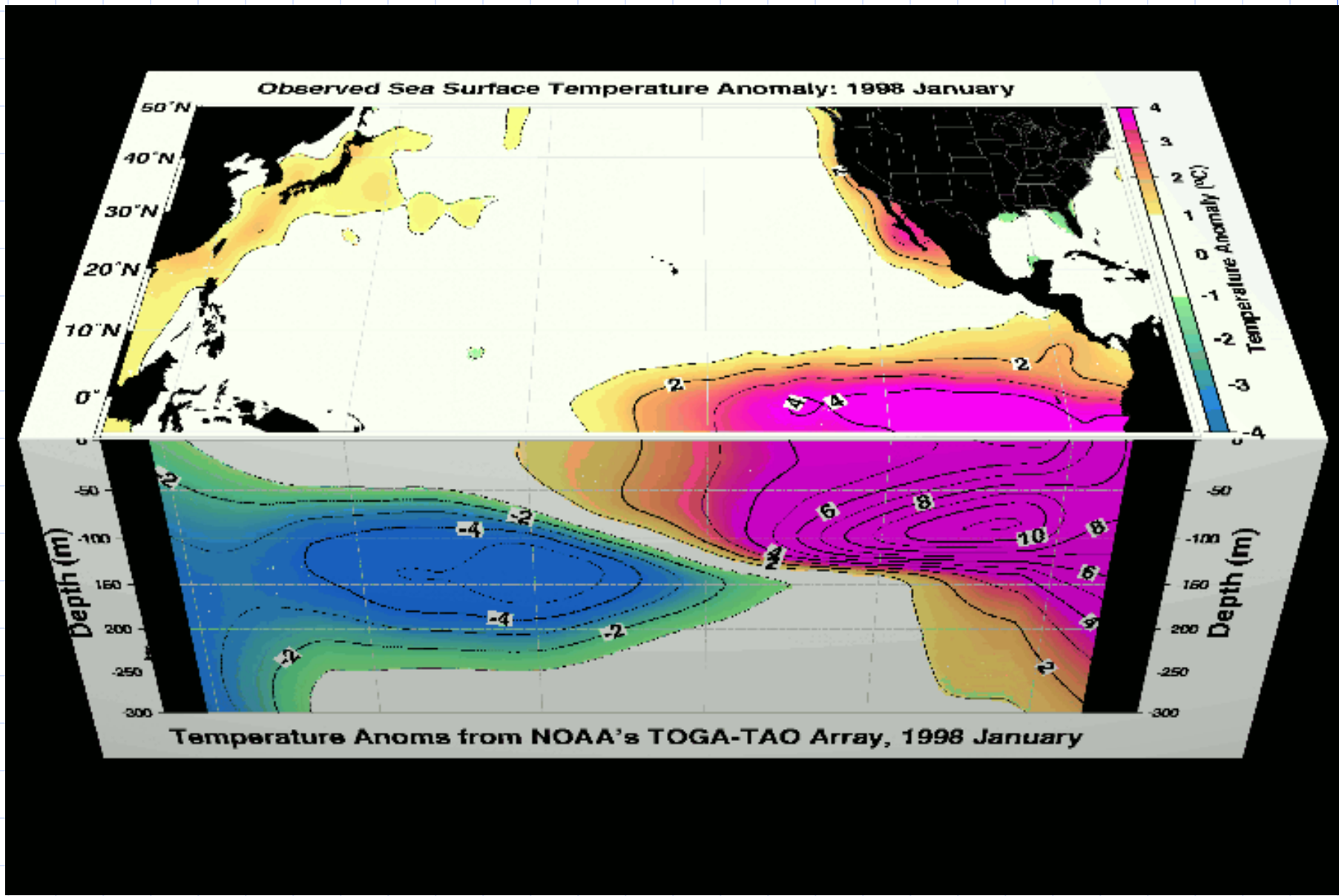


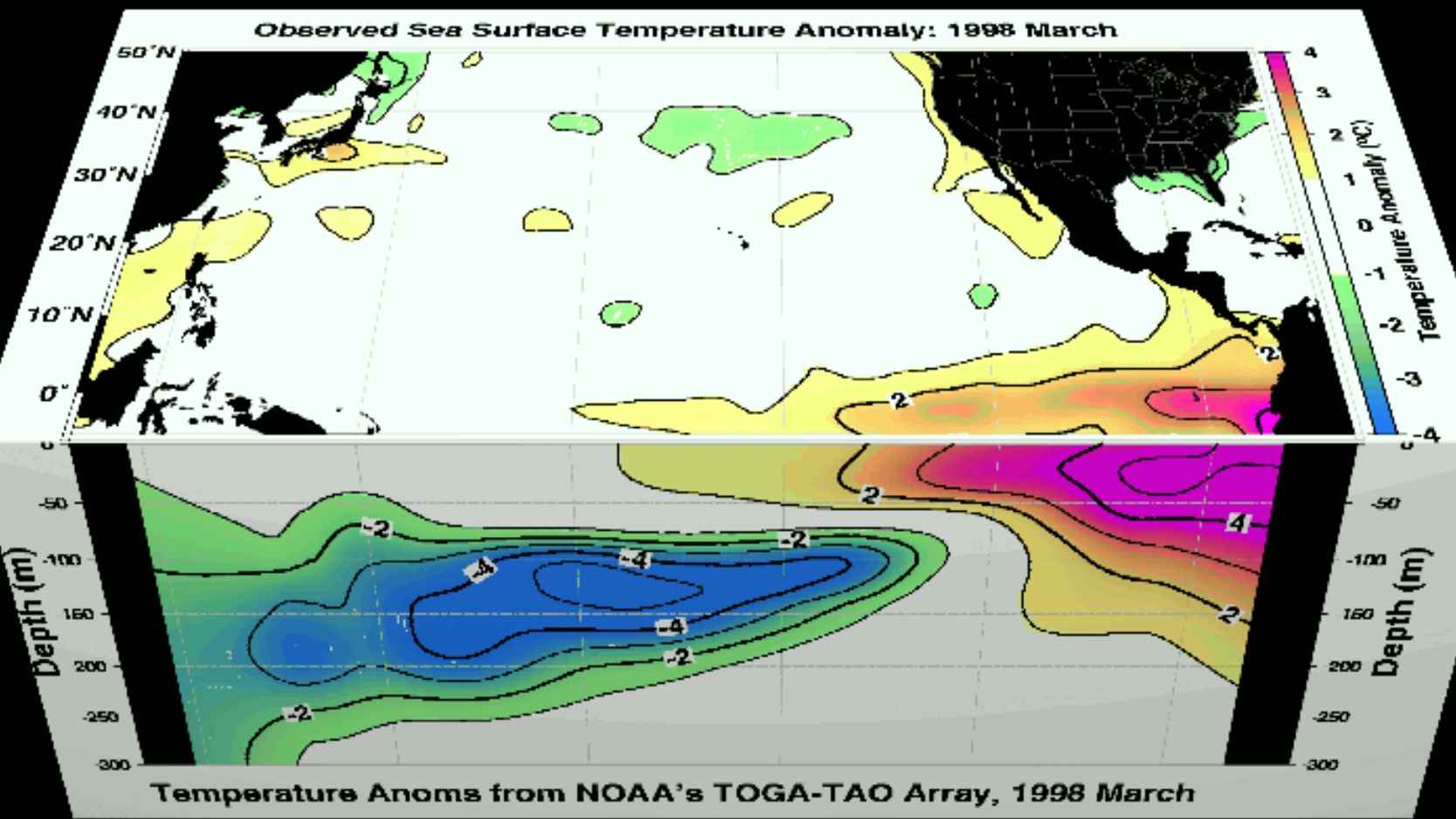


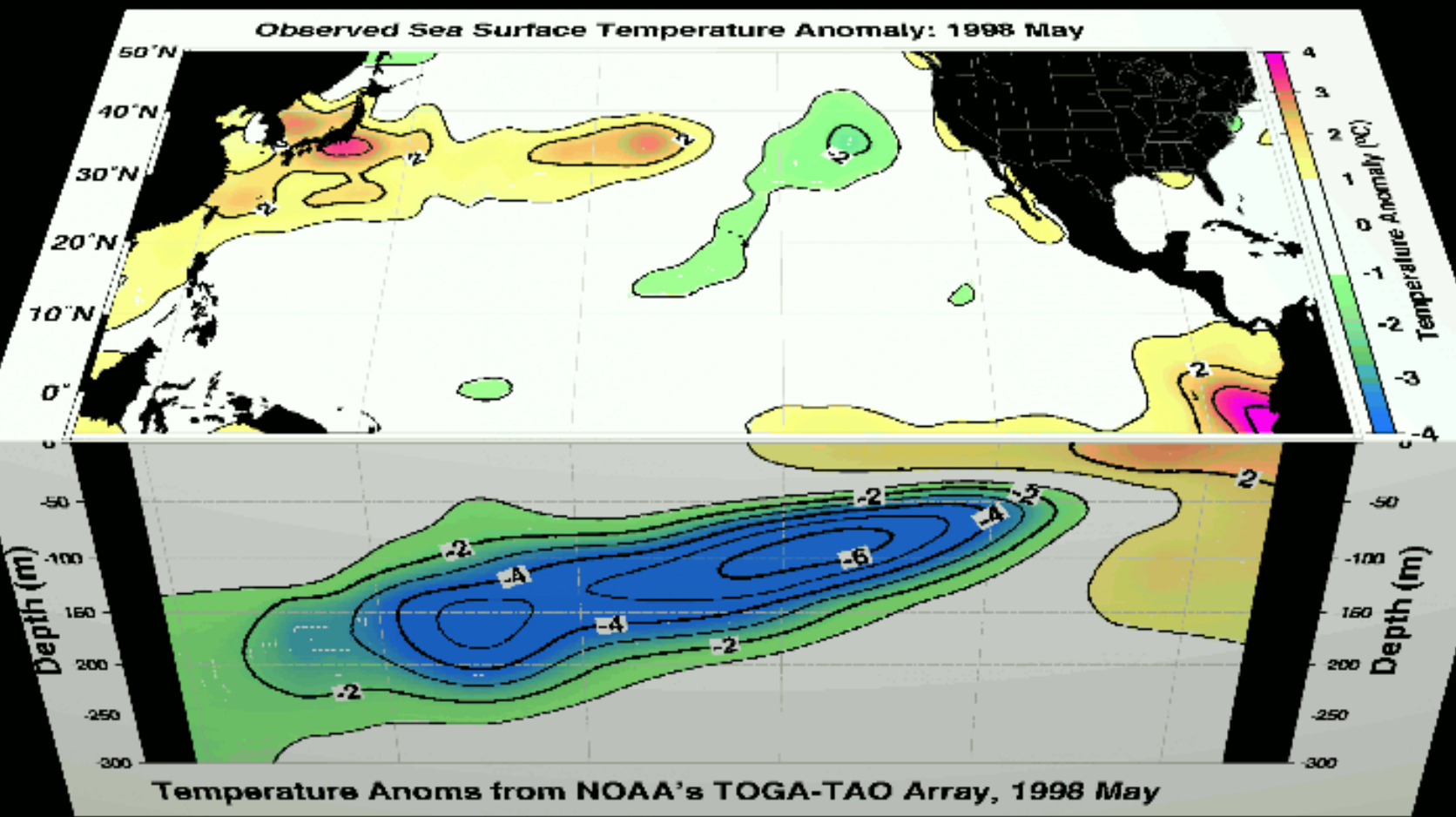
Observed Sea Surface Temperature Anomaly: 1997 May











Summary of major characteristics of the ENSO

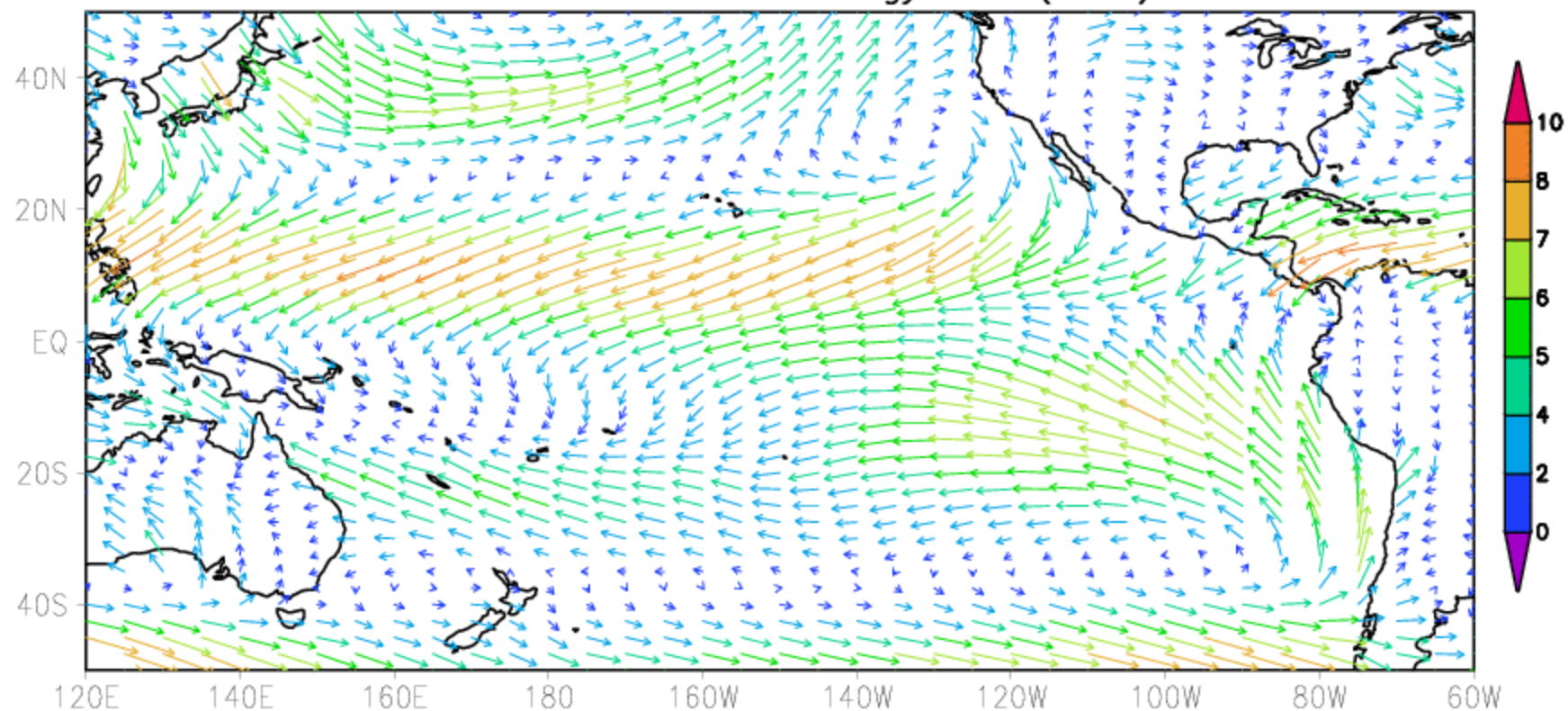
- The SST variations (Nino) are strongly correlated with the pressure seesaw (SO).
- Phase locked with Annual cycle
- El Nino and La Nina events tend to alternate about every three to seven years. However, the time from one event to the next can vary from one to ten years.
- The strength of the events, as judged by the SOI anomaly or Nino-3 anomaly, varies greatly from case to case. The strongest El Ninos in this record occurred in 1982-83 and 1997-98 (The effects of 1982-1983 included torrential storms throughout the southwest United States and Australia's worst drought this century).
- Sometimes El Nino and La Nina events are separated not by their counterparts, but by rather normal conditions.

Understanding the ENSO phenomenon...

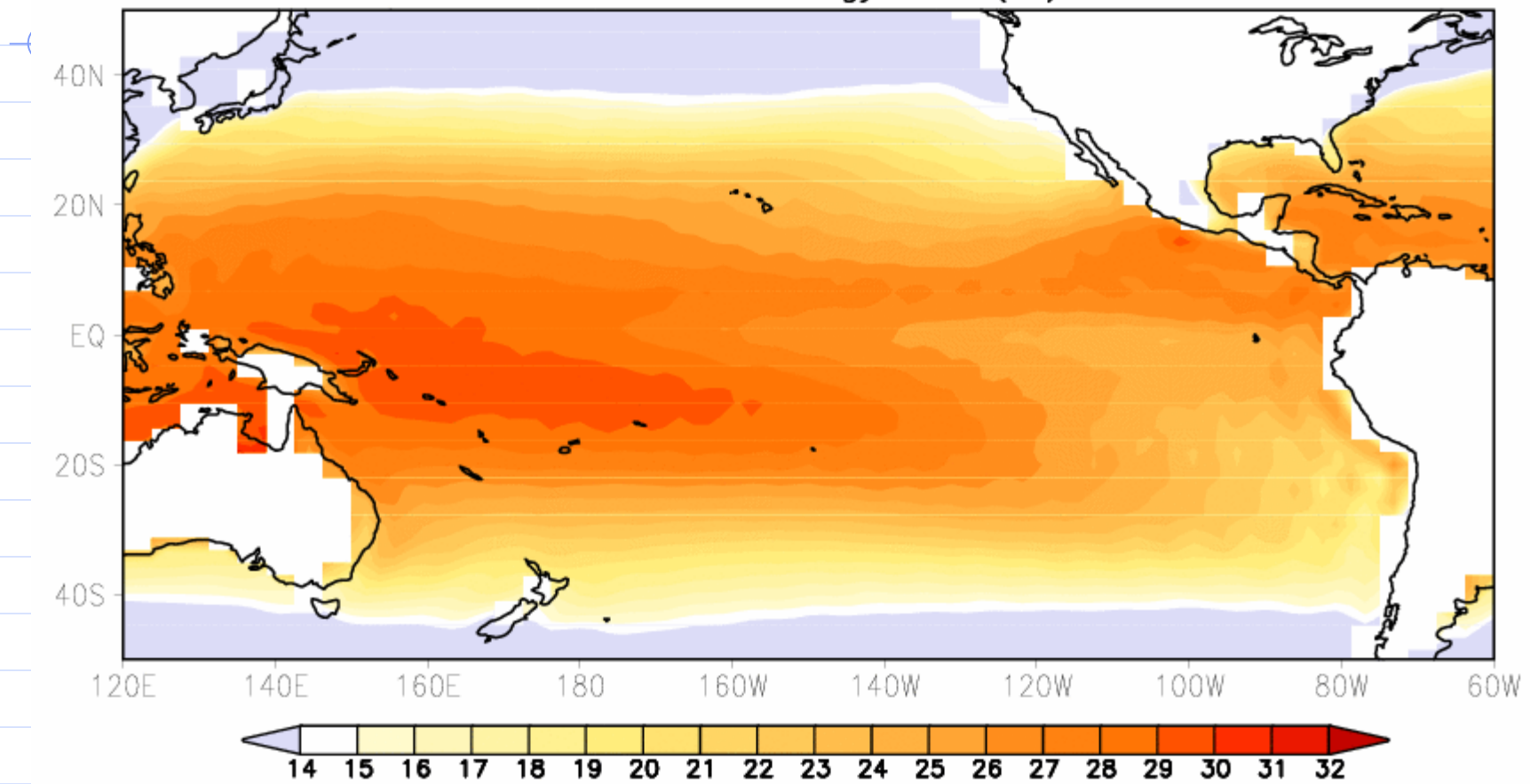
To understand these unusual events, let us first examine the prevailing normal (mean) conditions in the Pacific.

- Mean surface winds during winter
- Mean SST during winter
- Mean structure of thermocline in the equatorial Pacific

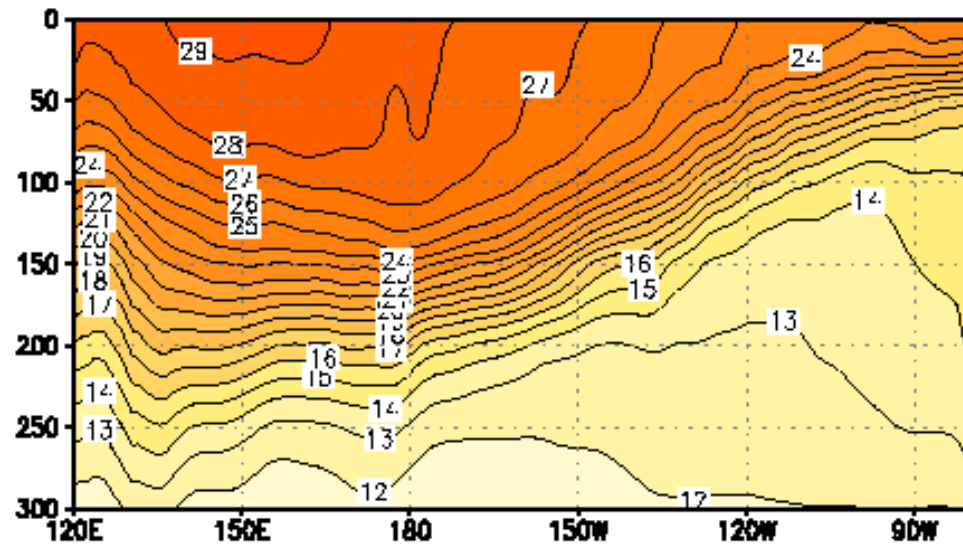
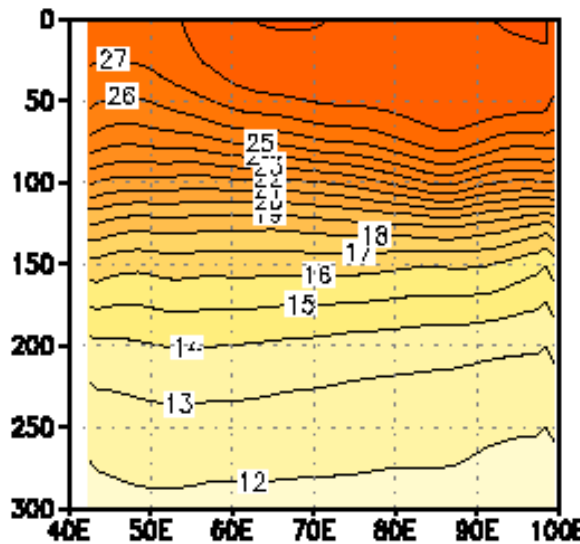
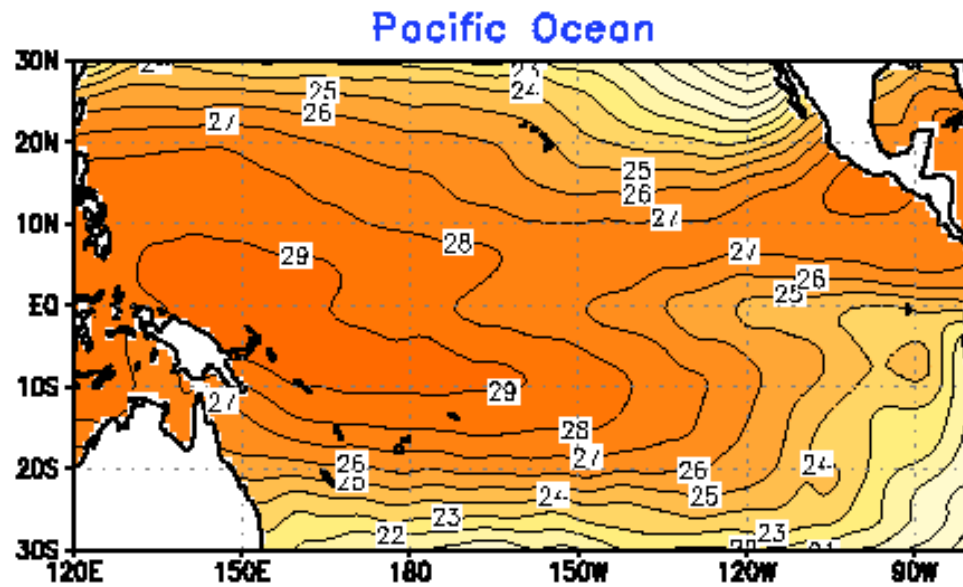
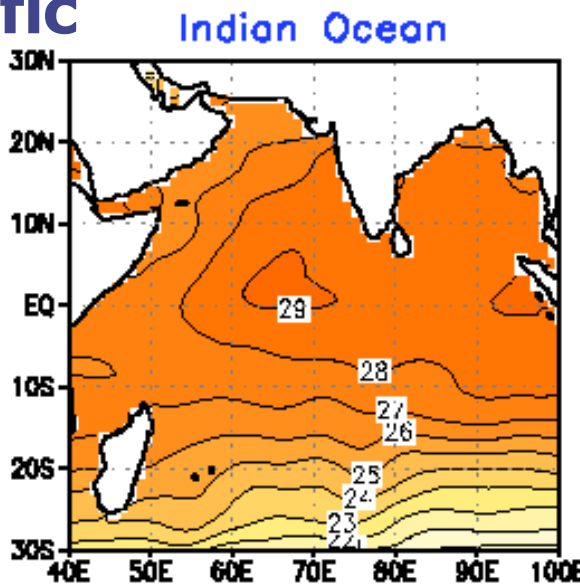
Surface Wind Climatology DJF (ms^{-1})



SST Climatology DJF (°C)



Contrasting SST and thermocline gradients over the IO and Pacific



Annual mean SST (top) and vertical cross section of temperature along the Eq.

The persistent easterly trade winds are a key ingredient in the ENSO process. They have two major effects:

- Pushing water toward the western Pacific. The sea level in the Philippines is normally about 60 centimeters (23 inches) higher than the sea level on the southern coast of Panama.
- Allowing the westward-flowing water to remain near the surface and gradually heat. This gives the water's destination—the western Pacific—the warmest ocean surface on Earth. Usually above 28°C (82°F), parts of this pool are sometimes as warm as 31.5°C (89°F).
- As warm surface water collects in the western Pacific, it tends to push down the thermocline, the boundary separating well-mixed surface waters from deeper, colder waters. The thermocline is usually about 40 meters (130 feet) deep in the eastern Pacific but varies from 100 to 200 meters (330-660 feet) deep in the west.

The clearest sign of the SO is the inverse relationship between surface air pressure at two sites: Darwin, Australia, and the South Pacific island of Tahiti. As seen in Figure 1, high pressure at one site is almost always concurrent with low pressure at the other, and vice versa. The pattern reverses every few years. It represents a standing wave or "see-saw", a mass of air oscillating back and forth across the International Date Line in the tropics and subtropics.

This two-dimensional picture was extended vertically by renowned meteorologist Jacob Bjerknes in 1969. He noted that trade winds across the tropical Pacific flow from east to west. To complete the loop, he theorized, air must rise above the western Pacific, flow back east at high altitudes, then descend over the eastern Pacific. Bjerknes called this the Walker circulation (in honor of Sir Gilbert Walker); he also was the first to recognize that it was intimately connected to the oceanic changes of El Nino and La Nina.

Bjerknes Hypothesis

Renowned meteorologist Jacob Bjerknes suggested in 1969 that the mean ocean and atmospheric circulation as well as the ENSO result from true coupling between the atmosphere and the ocean.

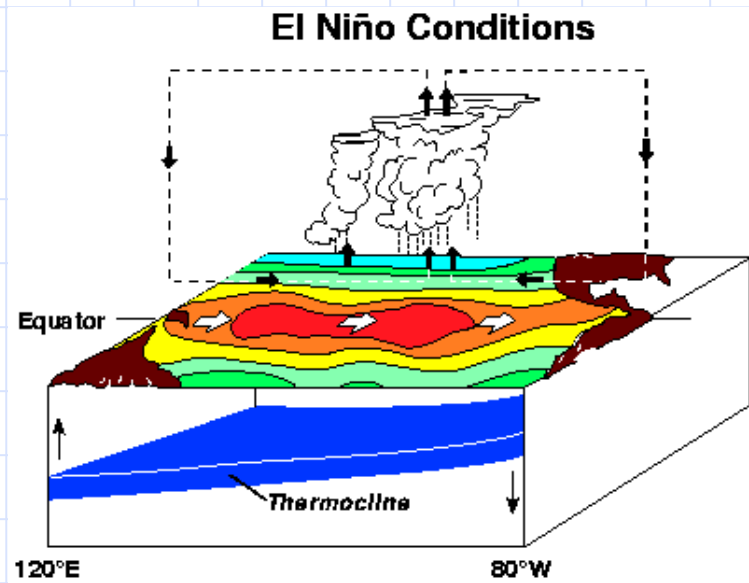
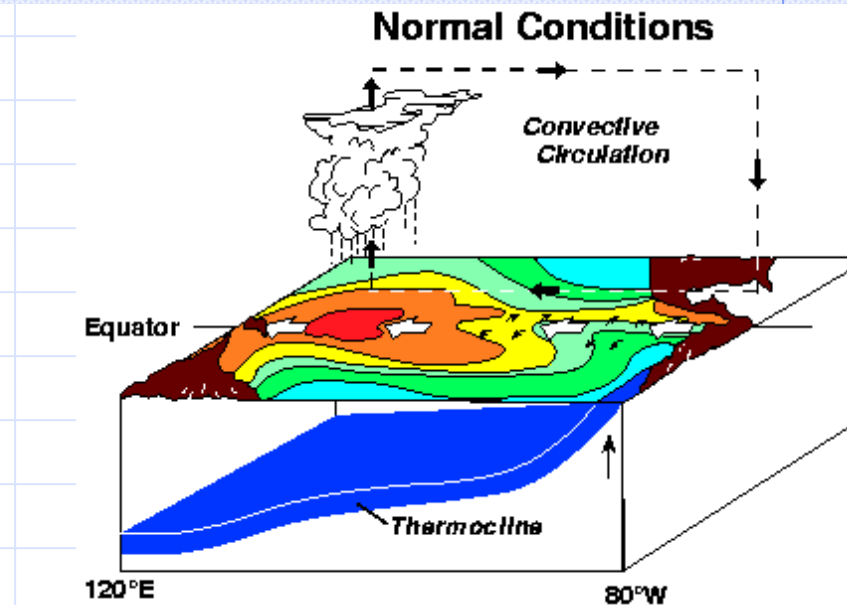
The persistent oceanic heat surrounding Indonesia and other western-Pacific islands leads to frequent thunderstorms and some of the heaviest rainfall on Earth. The rainfall is abetted by the upward motion produced by the Walker circulation.

The distribution of SSTs drives the enhanced rainfall, Walker circulation, and associated trade winds, which in turn are responsible for the ocean currents and maintain the east-west gradient of SSTs. The atmosphere drives the ocean and the ocean drives the atmosphere in a truly coupled mode of behavior.

(Top) How SST drive Walker Circulation winds → that maintain SST distribution & easterlies in the Mean

(bottom) El Niño Development

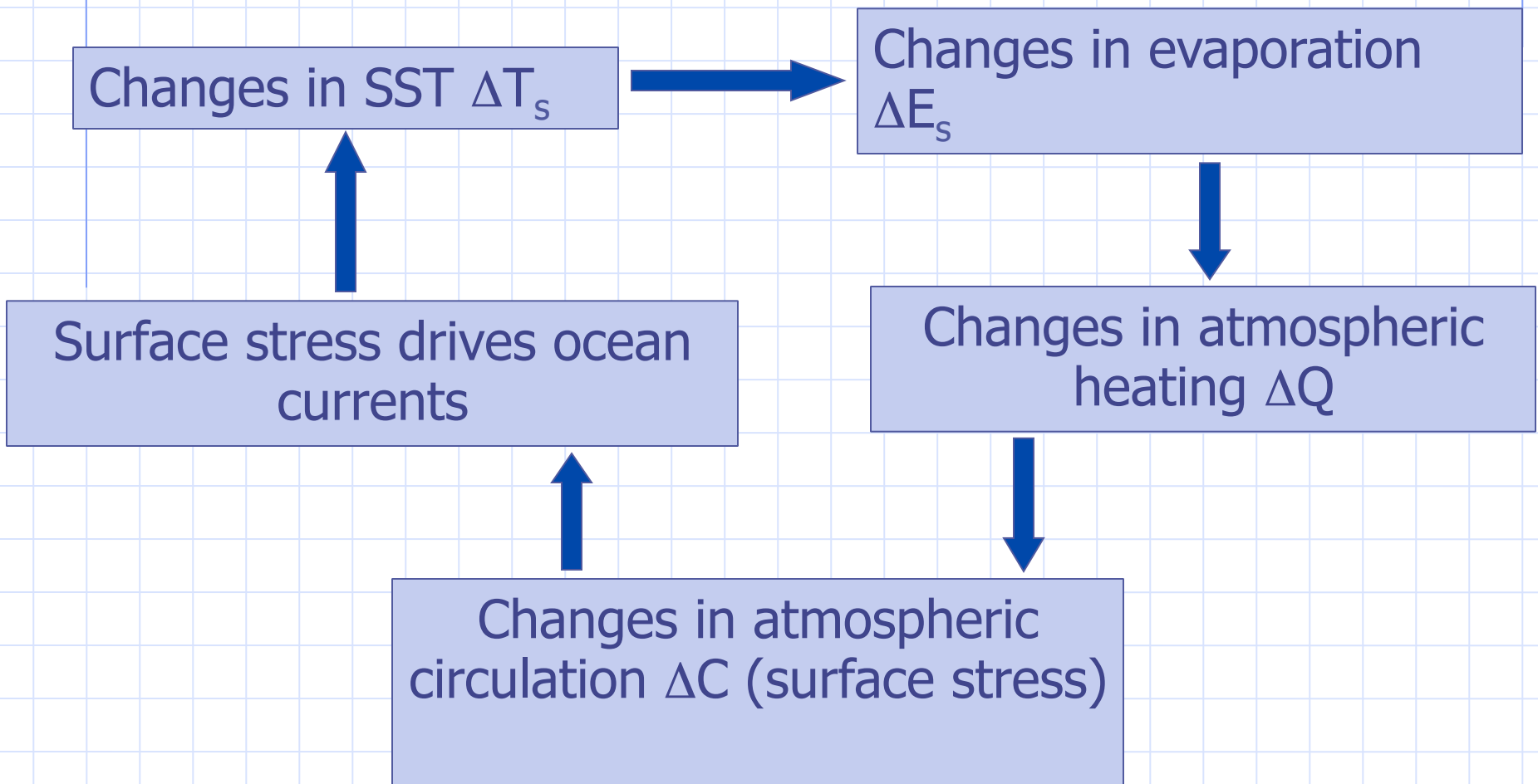
A westerly wind burst → weaken the mean easterly in WP → Cannot maintain the EW pressure gradient → the warm pool expands a bit eastward → Centre of rainfall & heating move eastward → westerly anomaly to the west of heating further weaken the easterlies → the warm pool and heat source move further east



→ Positive feedback

Air-sea interaction theory of ENSO

How does atmosphere and ocean interact in the tropics?



Where is this Air-sea Interactions most Effective? **TROPICS**

For this,

Small Change in SST → large change in moisture availability. High mean SST in tropics makes it possible. Low SST in middle lat makes it less effective

Available moisture → should result in latent heat release. Conditionally unstable thermal structure makes it possible in the tropics. A stable atmosphere in extra-tropics makes it less effective for converting moisture to heating

Why large scale air-sea interactions are more favourable in the tropics on interannual time scales?

- The free equatorial Kelvin wave and Equatorial Rossby wave have group and phase speed that is much larger in the equatorial region. Therefore, redistribution of SST could take place in the tropics on seasonal to interannual time scale.
⇒ In the middle latitude open ocean adjustment is only through the Rossby wave and the Rossby wave could take a long time to cross basin like Pacific. Adjustment time very large.
- The tropical atmosphere is conditionally unstable. Therefore, the available moisture could be easily converted to heating.

An example of travel time of disturbance in an Equatorial Ocean

Let c = Characteristic period of the first baroclinic mode $\approx 2.0\text{ms}^{-1}$

t = time taken by the Kelvin wave to travel a distance x and a reflected Rossby wave to travel a distance x .

$$= \frac{x}{c} + \frac{x}{\frac{c}{3}} = \frac{4x}{c} \approx \frac{7.5 \times 10^6 \text{m}}{2\text{ms}^{-1}} \approx 5.6 \text{months}$$

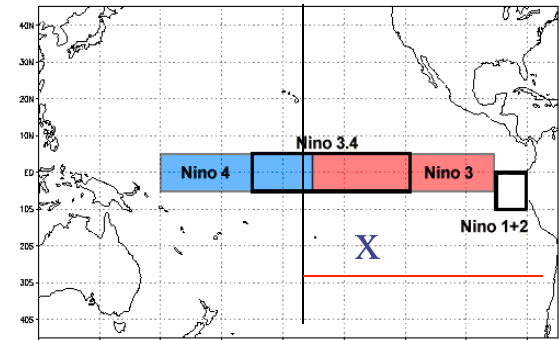
Extratropical Ocean

In the extratropics, the disturbance can be carried only by the Rossby wave. The gravest Rossby wave here has phase speed

$$c_r = \frac{\beta c^2}{f^2} \approx \frac{c^2}{(\beta y^2)}$$

Let us just calculate the time taken by such a Rossby wave to cross the basin at $y = 20^\circ\text{N} \approx 2000\text{km}$.

$$t = \frac{x}{c_r} = \frac{x\beta y^2}{c^2} \approx 4.8 \text{ years}$$



DYNAMICS OF SIMPLE COUPLED MODELS

An instability of
the coupled
system is
needed to
explain ENSO
amplitude.

→ Is the
Tropical coupled
Ocean-
Atmosphere
unstable?

First baroclinic mode Atmosphere

$$\frac{\partial U}{\partial t} - \beta y V + \frac{\partial \phi}{\partial x} + AU = 0$$

$$\frac{\partial V}{\partial t} + \beta y U + \frac{\partial \phi}{\partial y} + AV = 0$$

$$\frac{\partial \phi}{\partial t} + c_a^2 \left(\frac{\partial U}{\partial x} + \frac{\partial V}{\partial y} \right) + B\phi = -Q$$

First baroclinic mode (or reduced gravity) Ocean

(I) **Ocean model**

$$\frac{\partial u}{\partial t} - \beta y v + g' \frac{\partial h}{\partial x} + au = \frac{\tau^x}{\rho_0 \bar{h}}$$

$$\frac{\partial v}{\partial t} + \beta y u + g' \frac{\partial h}{\partial y} + av = \frac{\tau^y}{\rho_0 \bar{h}}$$

$$\frac{\partial h}{\partial t} + \bar{h} \left(\frac{\partial u}{\partial x} + \frac{\partial v}{\partial y} \right) + bh = 0$$

$$T = \kappa h \text{ and } Q = \alpha h$$

(II) Second Ocean model

$$\frac{\partial u}{\partial t} - \beta y v + g' \frac{\partial h}{\partial x} + au = \frac{\tau^x}{\rho_0 \bar{h}}$$

$$\frac{\partial v}{\partial t} + \beta y u + g' \frac{\partial h}{\partial y} + av = \frac{\tau^y}{\rho_0 \bar{h}}$$

$$\frac{\partial h}{\partial t} + \bar{h} \left(\frac{\partial u}{\partial x} + \frac{\partial v}{\partial y} \right) + bh = 0$$

$$\frac{\partial T}{\partial t} + \bar{T}_x u - K_T h + dT = 0$$

where $Q = \alpha T$, K_T is an entrainment factor.

\bar{T}_x — mean SST gradient in the SW. $\tau^x = \beta u$, $\tau^y = \beta v$

The growth rate (thick curve ,top) and real frequency (middle) of the unstable mode in the coupled model – III. The unstable mode has very slow eastward phase speed (almost stationary). The bottom panel shows the horizontal structure of the unstable mode.

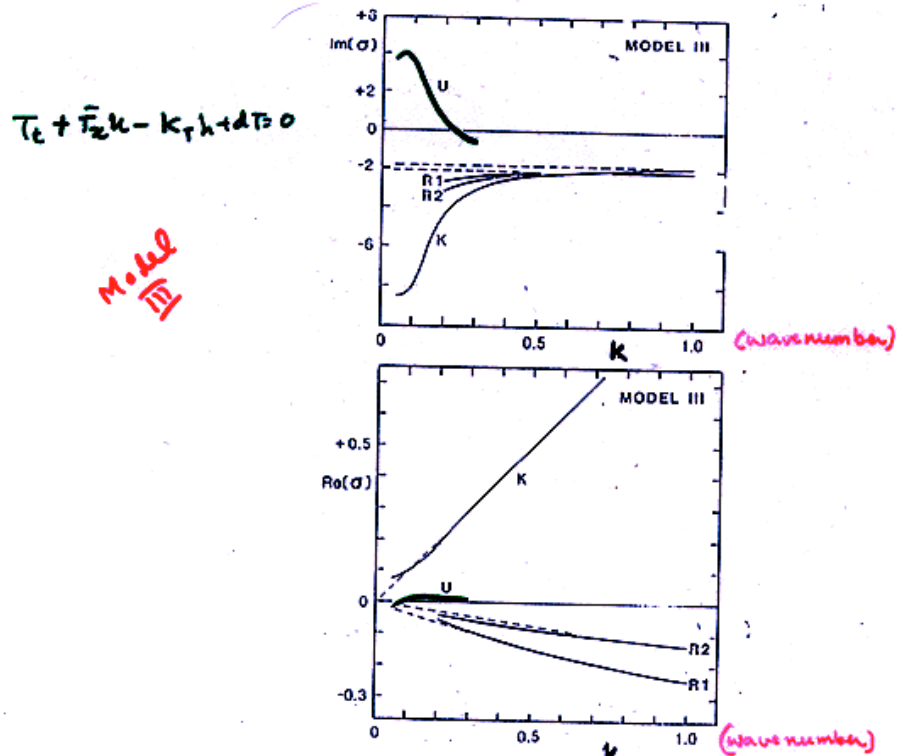


FIG. 13. As in Fig. 12 but as functions of wavenumber k .

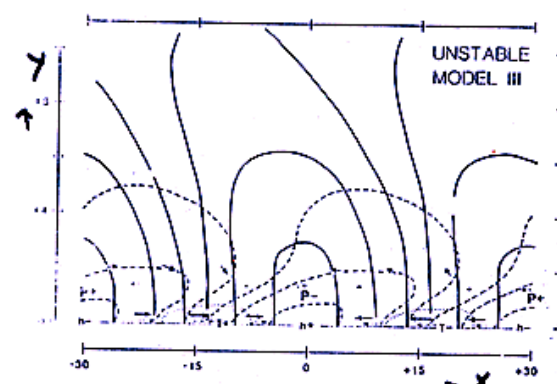


FIG. 14. Eigenfunction for the Model III unstable mode when K_0 and K_1 have "representative" values; otherwise as for Fig. 5.

HIRST'S MODEL-III WHERE BOTH UPWELLING AND ADVECTION ARE INCLUDED. PARAMETER REPRESENT CENTRAL PACIFIC BUT STRONGER THAN CLIMATOLOGY BY A FACTOR OF TWO.

A.C. Hirst, 1986: J. Atmos. Sci., 43, 606- 630

ENSO - Theory

- ◆ How does the phase of ENSO reverse?
- ◆ What determines the ~4 year periodicity
- ◆ What triggers an El Nino event?

What determines the 4-year periodicity?

Power Spectrum

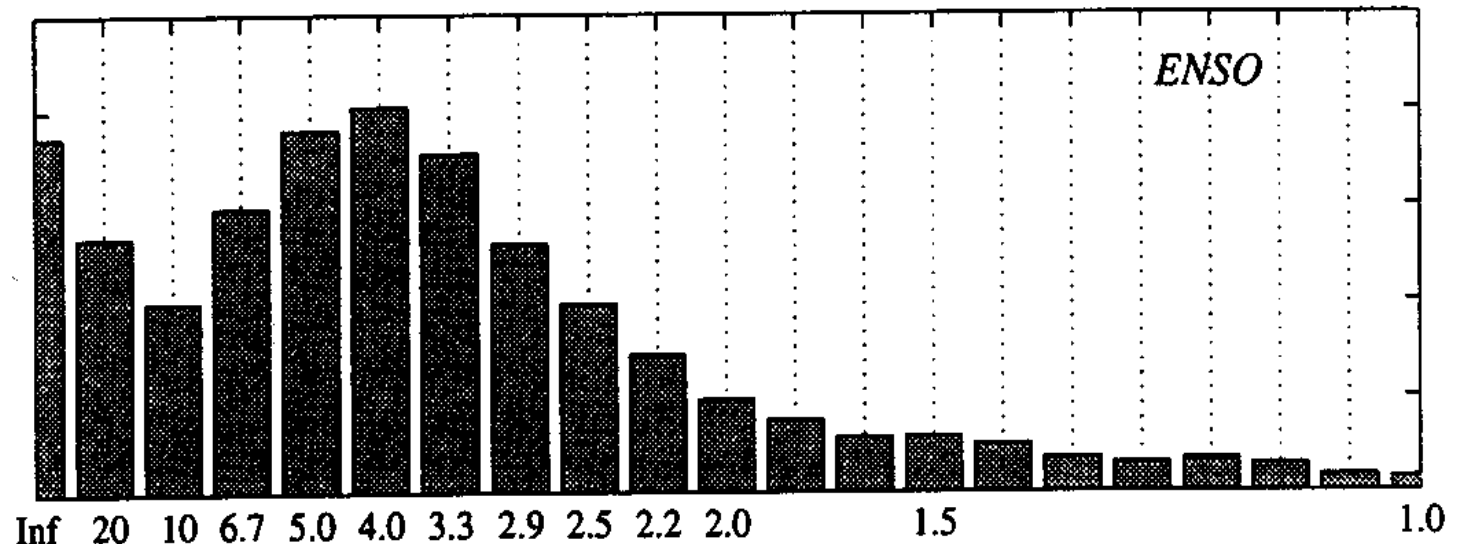


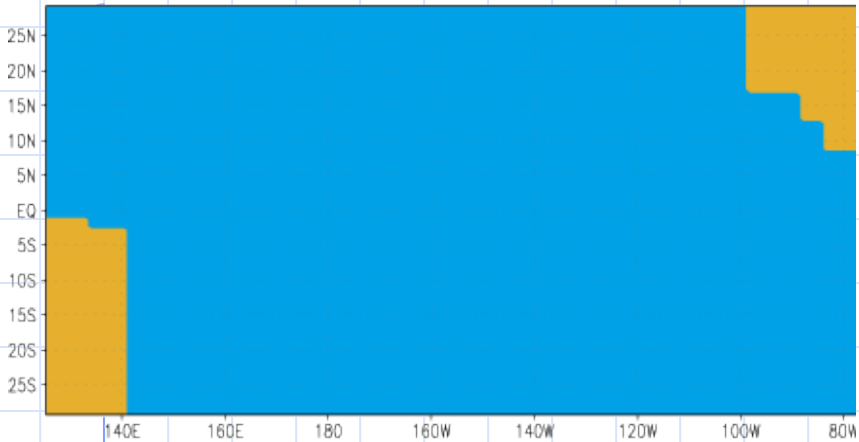
Figure 9: Power spectra of (top panel) equatorial Pacific SST (the time series is based on twice-yearly data for 1882-1992).

Equatorial Waves

- ◆ Equatorial waves in the ocean are believed to play an important role in the onset and variability of ENSO
- ◆ Two types:
 - Kelvin waves (propagate eastward along the equator and also along coasts)
 - Rossby waves (long waves propagate westward)
- ◆ The relevant waves are baroclinic: internal to the ocean, propagating along the density contrast of the thermocline
- ◆ Equatorial Kelvin waves travel 3 times faster than the fastest equatorial Rossby waves

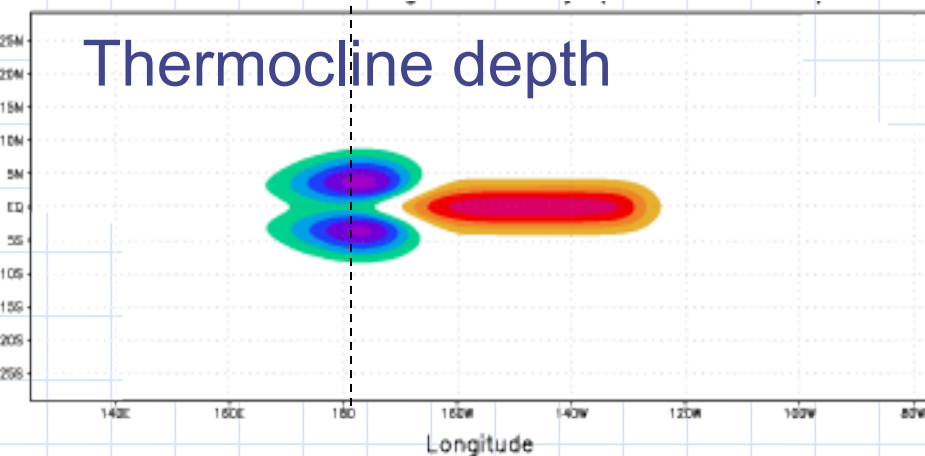
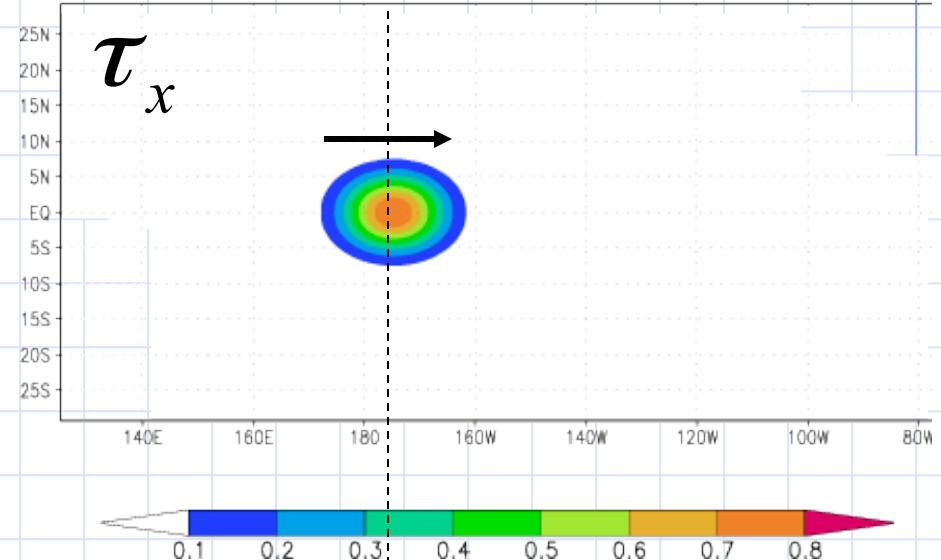
How does the phase of ENSO reverse?

Delayed Oscillator Theory

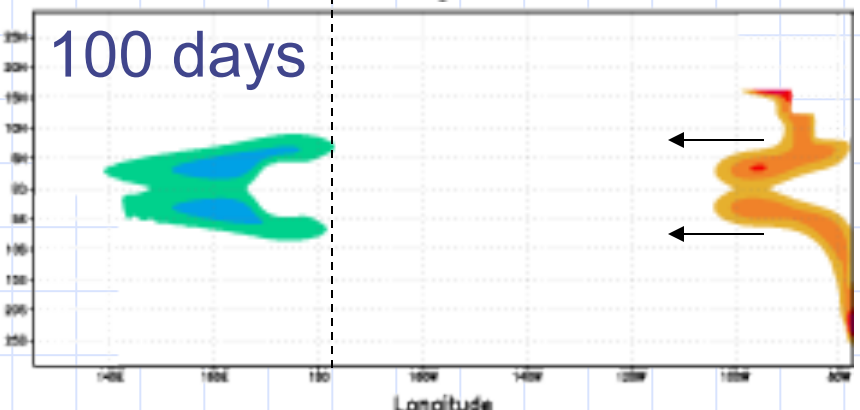
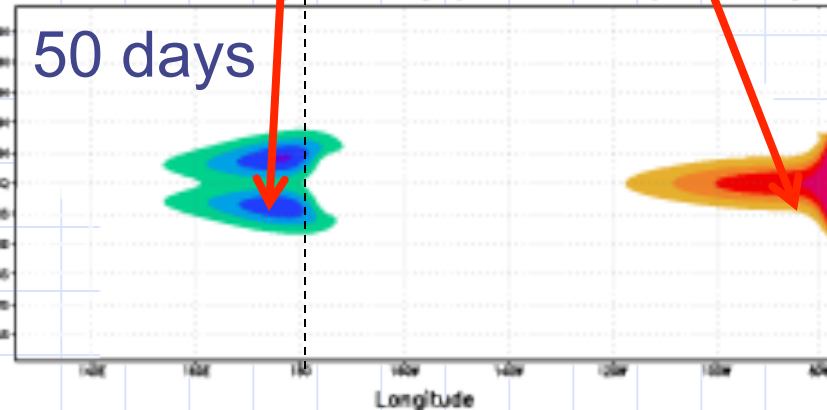
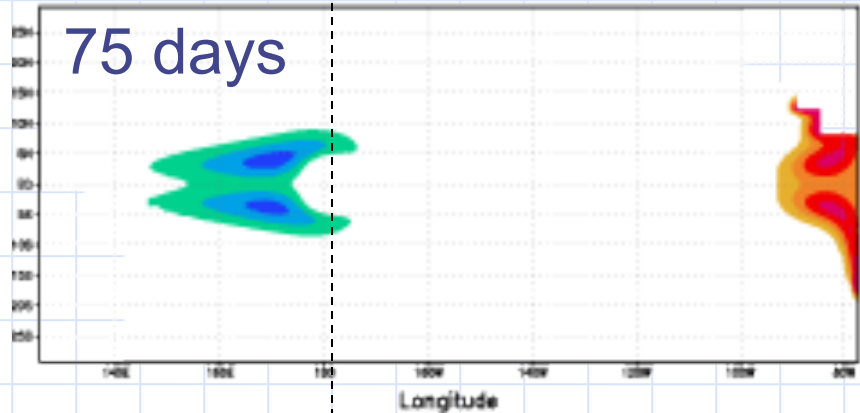
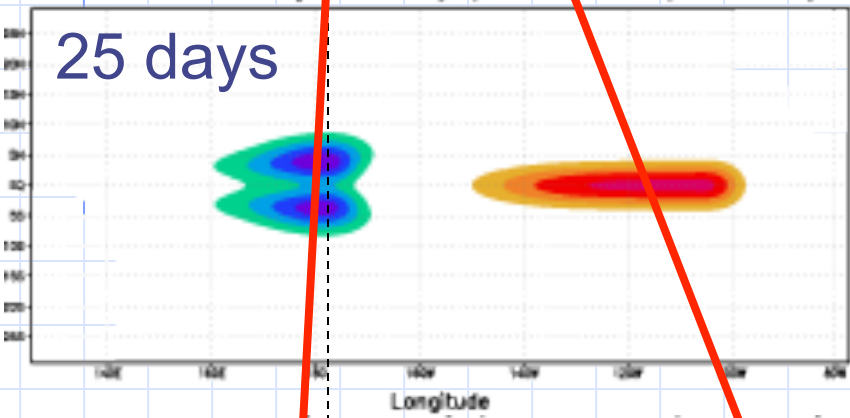
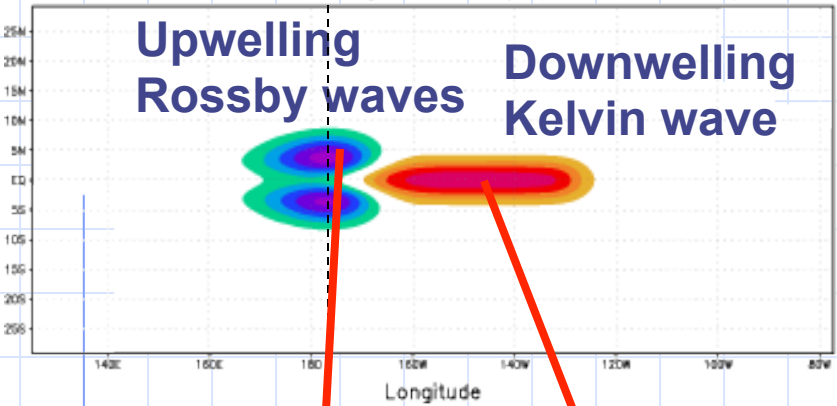


- Westerly winds force downwelling on Equator and upwelling to North and South
- => Excites Kelvin and Rossby waves

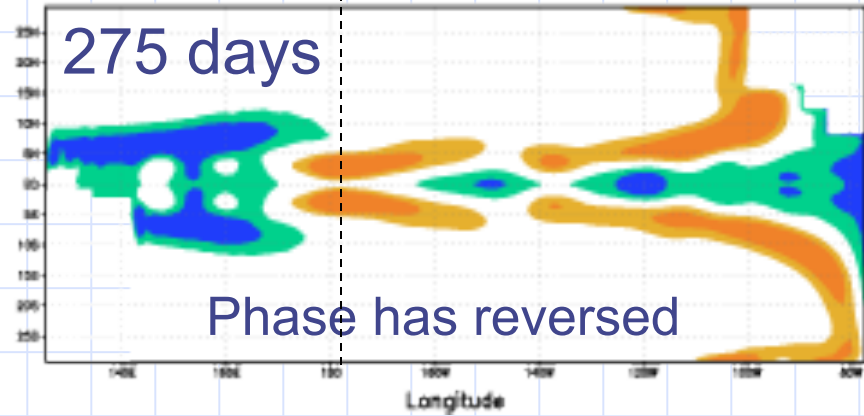
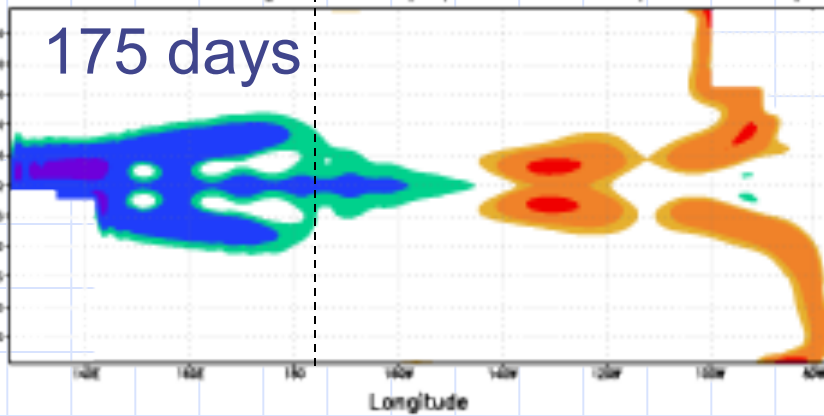
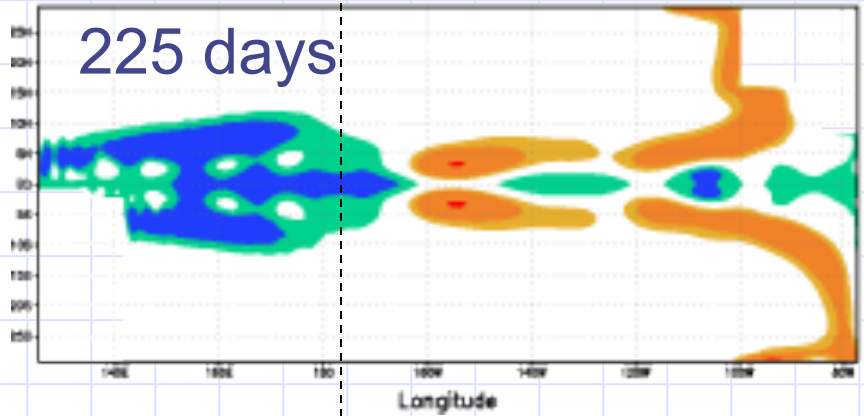
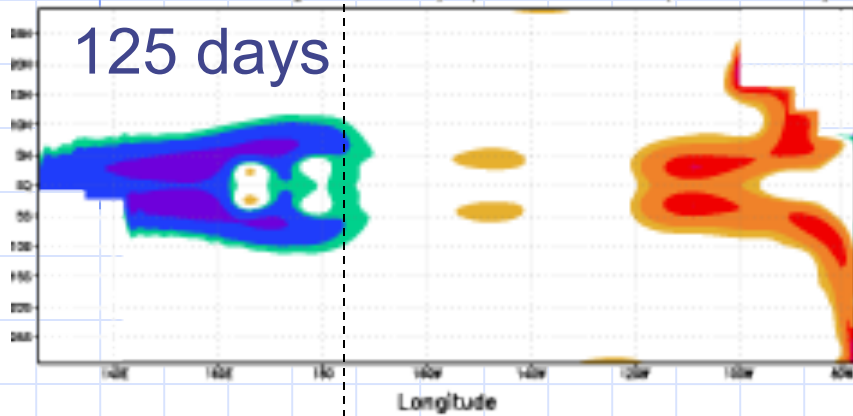
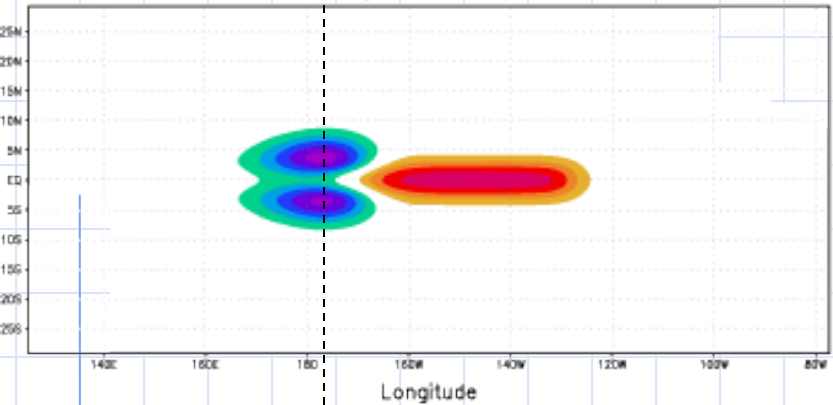
Battisti and Hirst, 1989; Suarez and Schopf, 1988



Delayed Oscillator Theory 2



Delayed Oscillator Theory 3



Delayed Oscillator Theory 4

- ◆ Equatorial ocean waves offer a mechanism to reverse the phase of perturbations to the thermocline depth
- ◆ Without further wind forcing waves eventually decay
- ◆ Thermocline depth perturbations influence SST in the upwelling regions of central / eastern equatorial Pacific => coupling to atmosphere
- ◆ Bjerkenes feedback + equatorial waves can generate a self-sustaining oscillation

Delayed Oscillator Theory of the ENSO



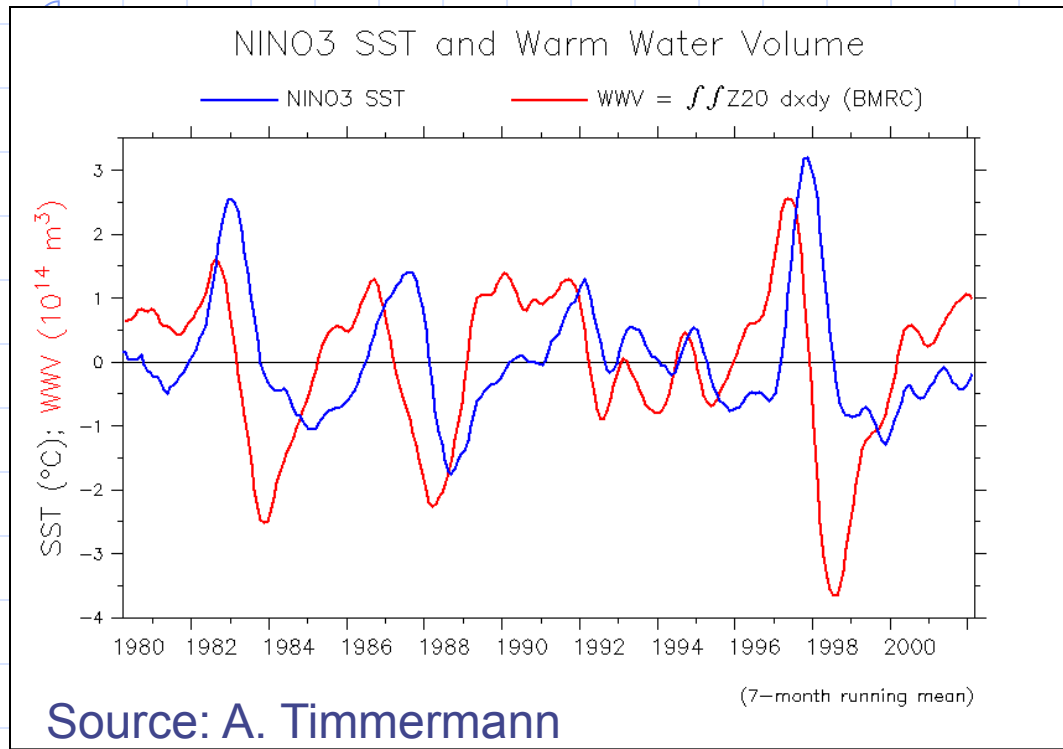
$$\frac{dT}{dt} = AT - BT(t - \eta) - \varepsilon T^3, \quad (1)$$

Coupled Instability, Bjeknes feedback

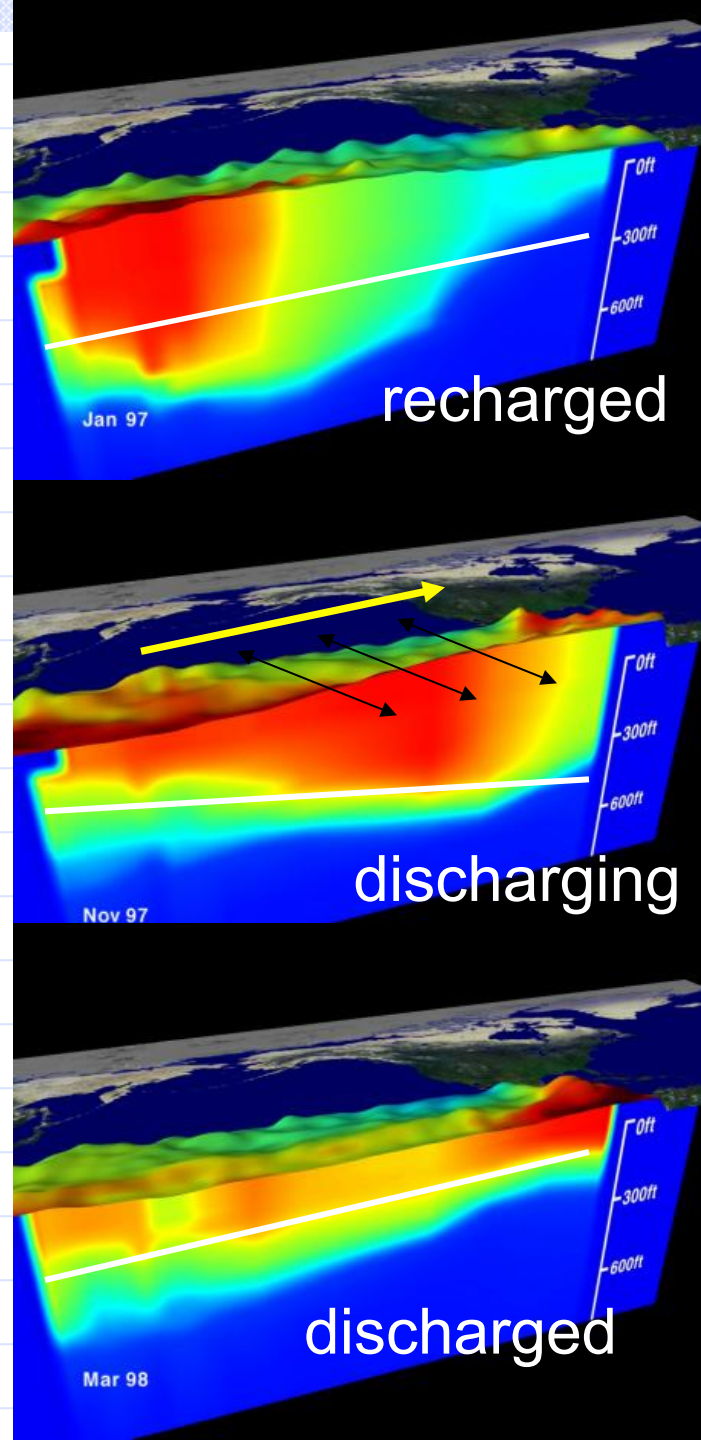
Delayed negative feedback

Nonlinearity associated with entrainment

Recharge/Discharge theory (Jin, 1997)



- Prior to El Nino heat content in equatorial region builds up
- During El Nino heat is “discharged” eastward and polewards



Recharge-discharge oscillator

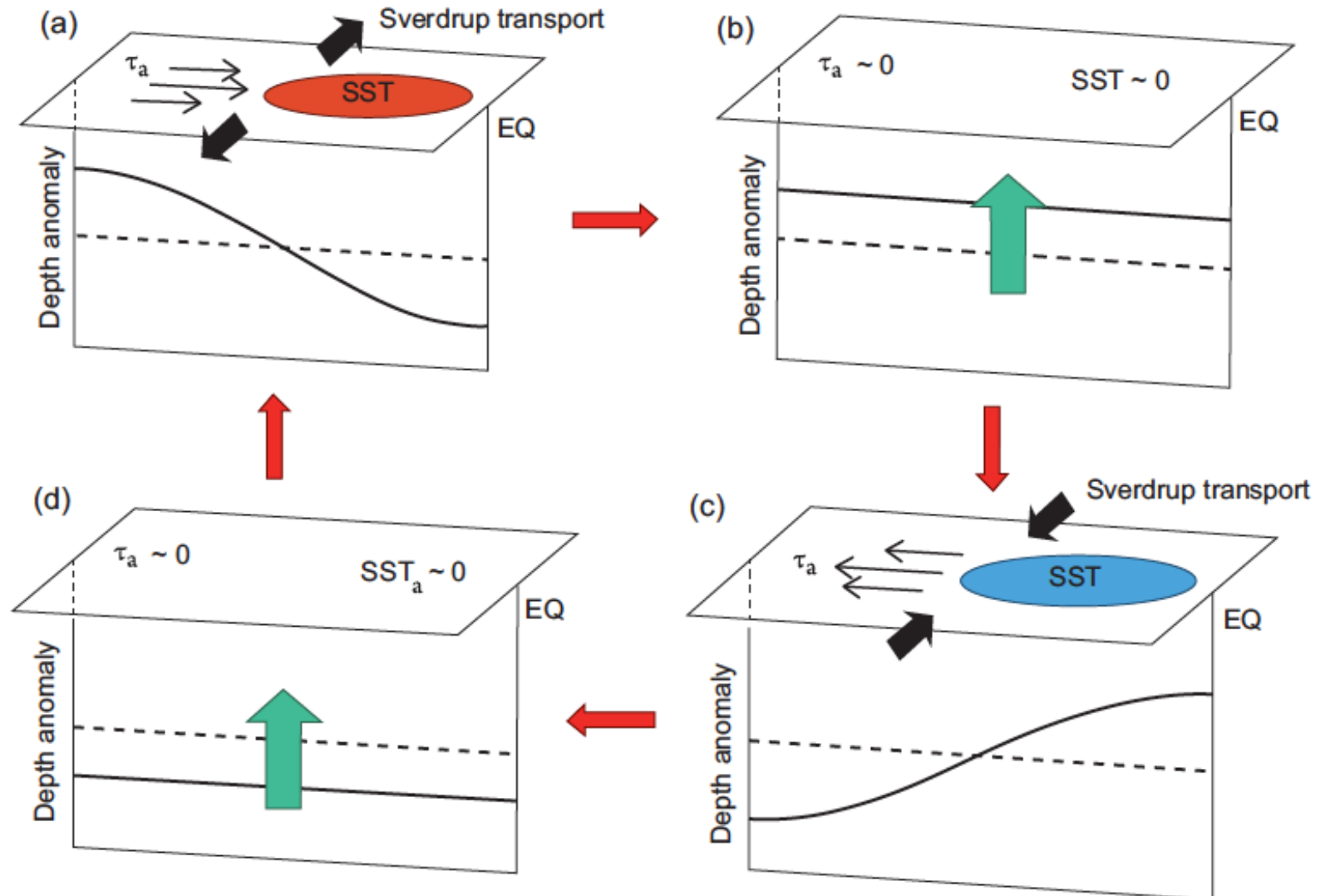
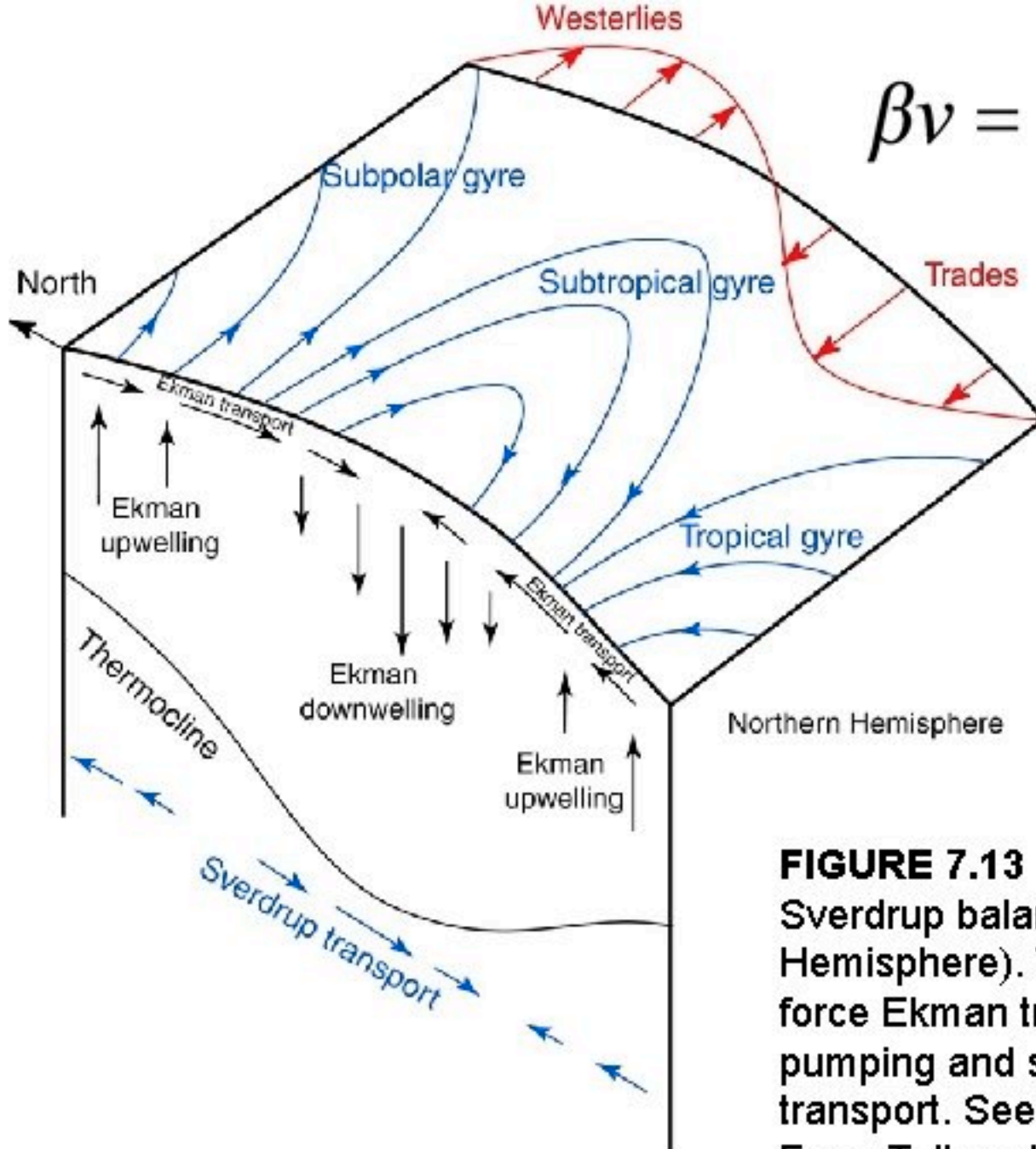


Figure 2. Schematic diagram of the recharge–discharge oscillator. Shown are (a) the warm phase, (b) the warm-to-cold transition phase, (c) the cold phase and (d) the cold-to-warm transition phase. Red (blue) SST represents warm (cold) SST anomalies and thin black arrows stand for wind anomalies. Dashed lines represent zero of the thermocline-depth anomalies and black lines are the thermocline-depth anomalies. Heavy black arrows mean the divergence and convergence of Sverdrup transport. Green arrows represent climatological mean upwelling.

$$\beta v = \frac{1}{\rho H} \left(\frac{\partial \tau_y}{\partial x} - \frac{\partial \tau_x}{\partial y} \right)$$



Have vorticity input

East

No vorticity dissipation

**Cannot hold everywhere
in a closed basin**

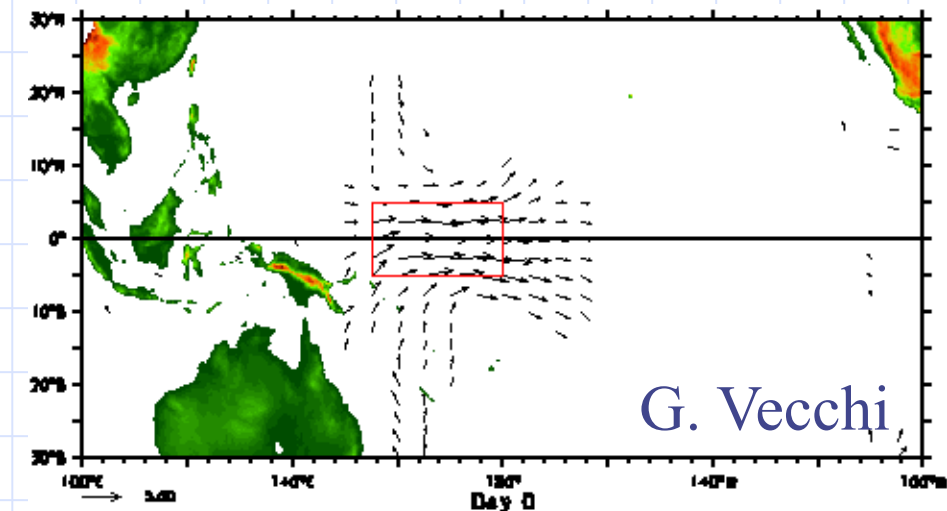
**Friction has to be
important somewhere
within the basin**

FIGURE 7.13

Sverdrup balance circulation (Northern Hemisphere). Westerly and trade winds force Ekman transport, creating Ekman pumping and suction and hence Sverdrup transport. See also Figure S7.12. From Talley et al(2011, PDO)

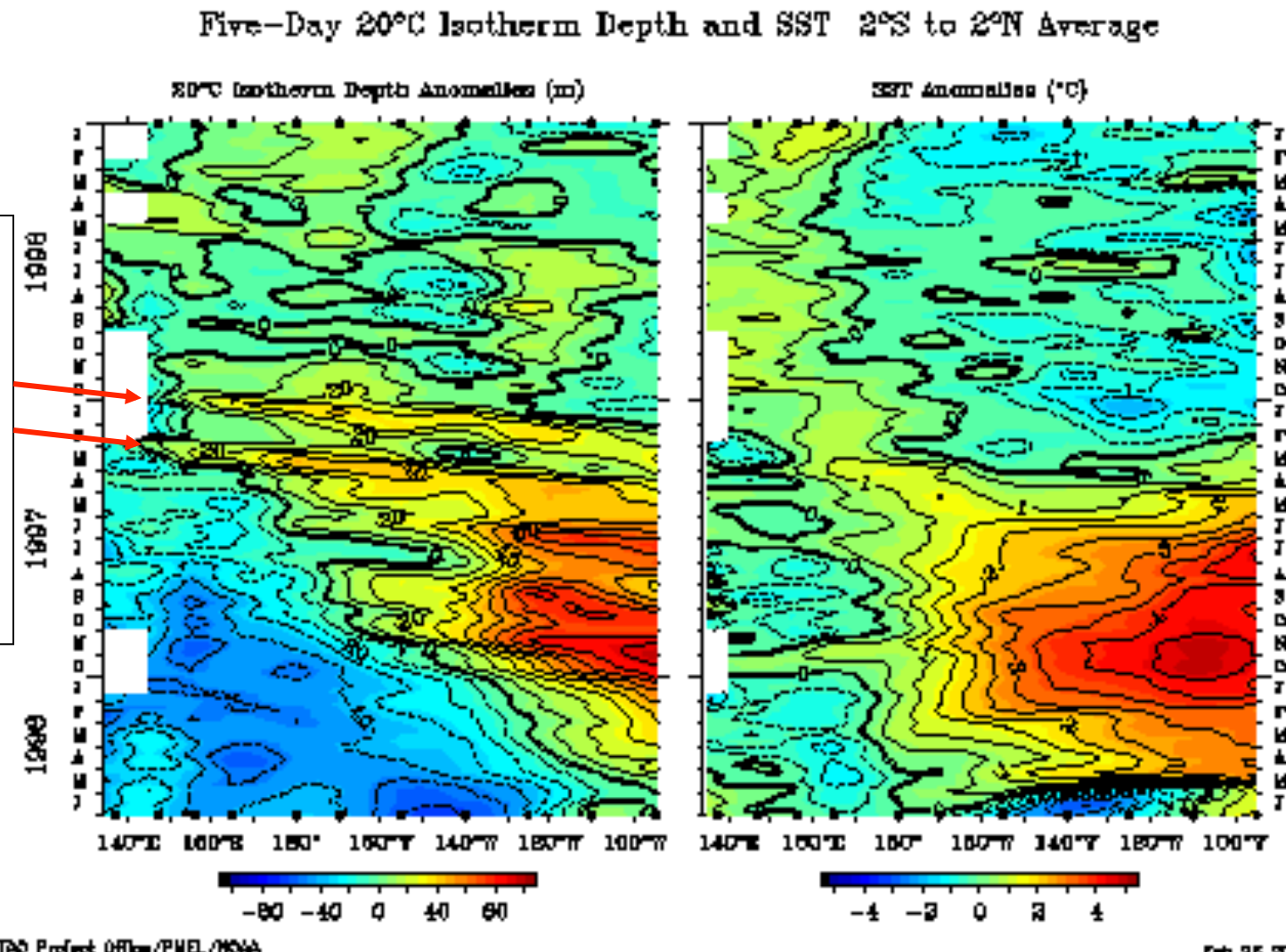
What triggers El Nino?

- ◆ Still not fully understood
- ◆ High heat content (deep thermocline) in the equatorial region necessary but not sufficient condition
- ◆ “Westerly wind bursts” (few days duration) associated with the Madden Julian Oscillation may act as one trigger.



Onset of the 1997/98 El Niño

Downwelling equatorial Kelvin waves triggered by westerly wind bursts



Summary of El Nino onset

- ◆ Need high heat content in equatorial Pacific
- ◆ Triggering by wind fluctuations (e.g. WWBs) over central/western Pacific
- ◆ Growth through Bjerknes positive feedback mechanism

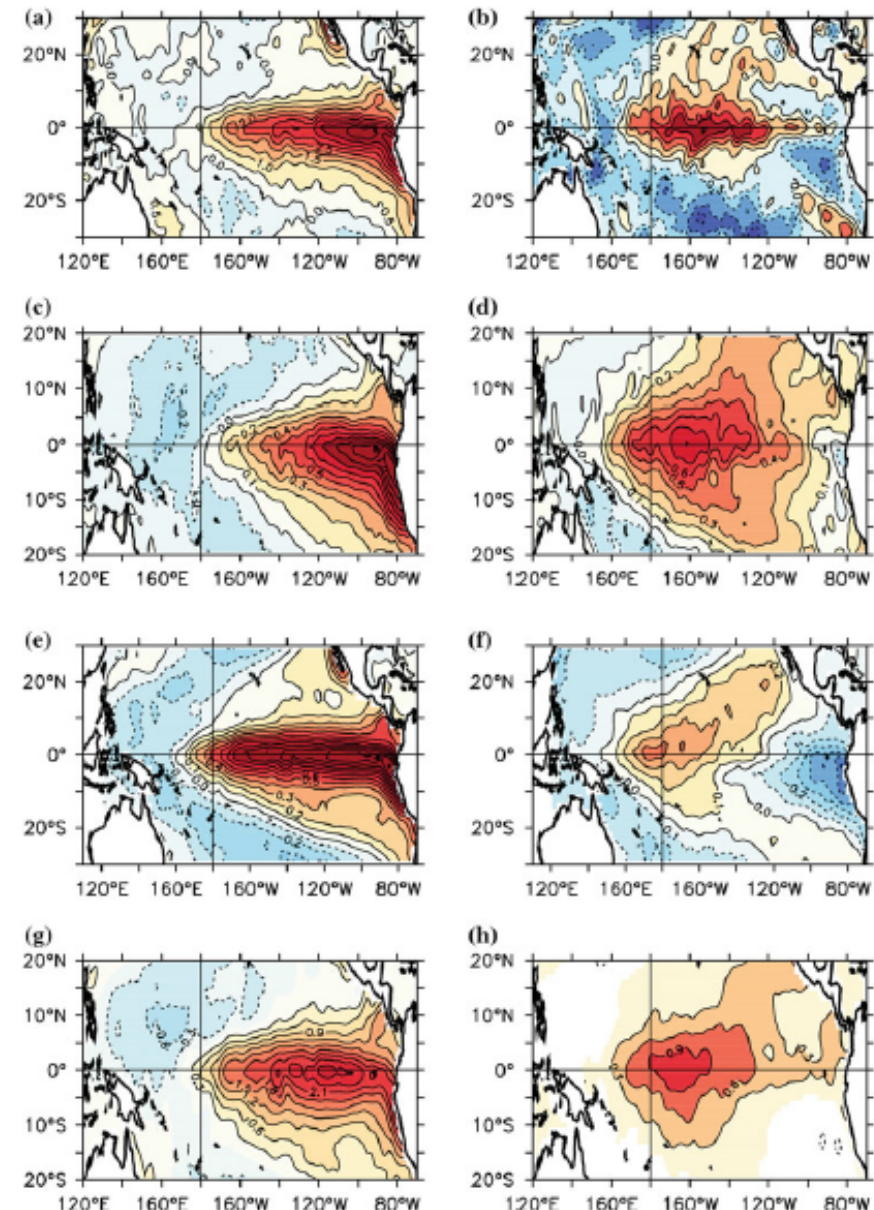
Theories for ENSO Oscillations

- ◆ **Delayed Oscillator** (e.g. Battisti and Hirst, 1989; Suarez and Schopf, 1988)
- ◆ **Recharge/discharge theory** (Jin, 1997)
- ◆ **Western Pacific Oscillator** (e.g. Weisberg, R. H., and C. Wang, 1997)
- ◆ **Advective-Reflective Oscillator** (e.g. Picaut et al, 1997)
- ◆ **Unified Oscillator** (Wang, 2001 J Clim)

Shades of ENSO

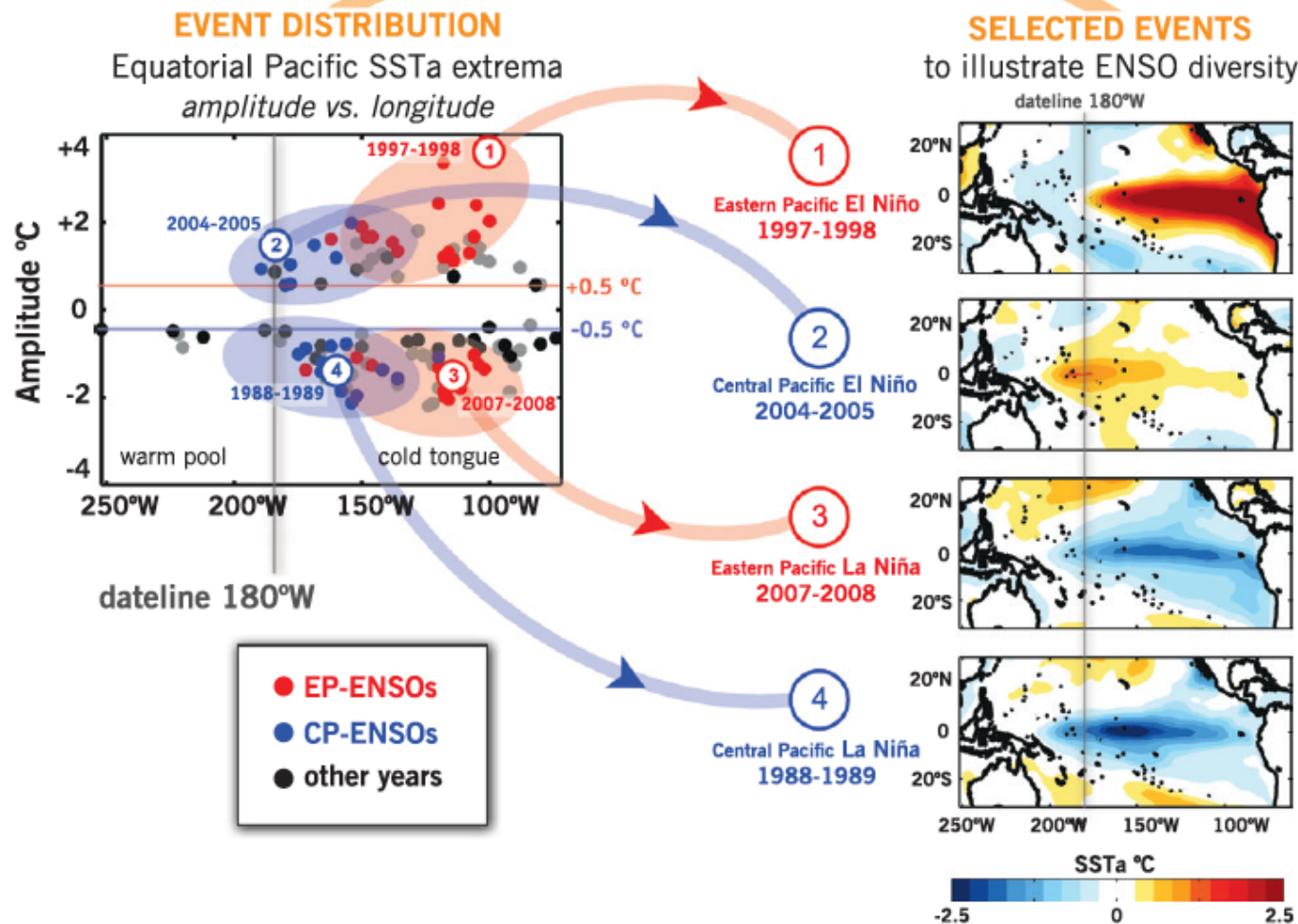
Fig. 4.4 SST anomaly patterns for a the 1997–98 El Niño (anomalies averaged from November 1997 to January 1998); b the 1977–78 El Niño (anomalies averaged from November 1977 to January 1978); c–d the EP-ENSO and CP-ENSO obtained from the EOF-regression method of Kao and Yu (2009); e–f the 1st and 2nd EOF that representing the conventional El Niño and El Niño Modoki obtained from the regular EOF analysis of Ashok et al. (2007); and g–h the Cold Tongue and Warm Pool El Niño composed by Kug et al. (2009). SST data from HadISST (1970–2005) were used in the calculation

One size does not fit all El Ninos! At least two ‘shades’ of El Ninos are known. The eastern Pacific (EP) El Nino and the Central Pacific (CP) El Nino. The spatial structure and evolutionary character of the two are different.



ENSO Diversity

Towards understanding and characterizing ENSO diversity



Capotondi et al., 2015: Understanding ENSO Diversity, BAMS

ENSO Complexity

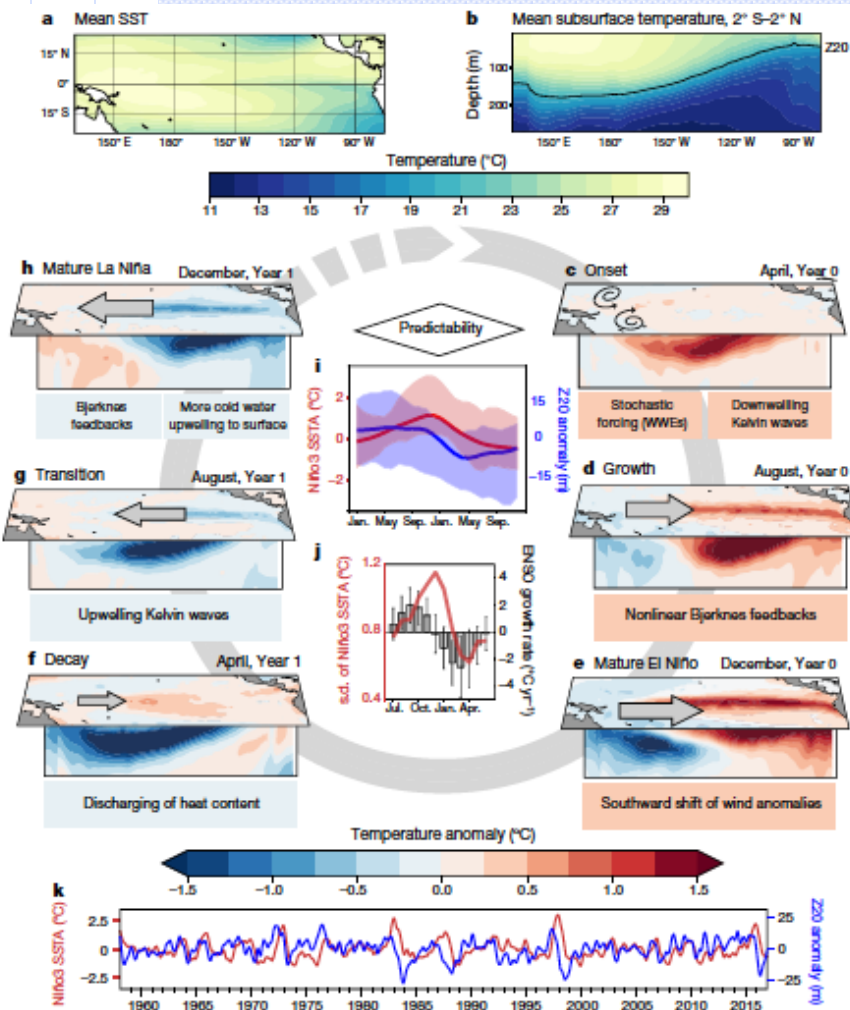


Fig. 1 | ENSO cycle. Composite evolution of El Niño events from 1958 to 2015. a, b, Mean SST²⁶ (a) and subsurface potential temperature²⁶ (b) between 2° N and 2° S. The depth of the 20 °C isotherm (Z20) is indicated by the black line. c–h, Composite SSTAs²⁶ and subsurface temperature anomalies²⁶ from 17 El Niño events (1963, 1965, 1968, 1969, 1972, 1976, 1977, 1982, 1986, 1987, 1991, 1994, 1997, 2002, 2004, 2006 and 2009), based on the 0.5 °C exceedance of the three-month running mean of the NOAA ERSST.v5 (Extended Reconstructed Sea Surface Temperature dataset, version 5) SSTAs³⁷ in the Niño3.4 region (averaged over 5° S–5° N and 120° W–170° W). The arrows represent wind anomalies and the boxes list major processes involved in the phases of El Niño evolution.

i, The seasonal composite means (lines) and spread (shading) of eastern equatorial Pacific SSTAs (red; averaged over the Niño3 region: 5° S–5° N and 90° W–150° W) and equatorial Pacific zonal mean Z20 (blue) for the 17 El Niño events. The diamond illustrates that ENSO predictability increases with increasing ENSO signal strength. j, The monthly standard deviation (s.d.) of the Niño3 SSTAs²⁶ (red line) and an estimate of the monthly ENSO growth rate based on the Bjerknes stability index. The error bars show the 90% confidence range for the index calculated from the standard error of the regression slope⁵⁶. k, Time series of the Niño3 SSTAs and zonal mean equatorial Pacific depth anomaly from the 20 °C isotherm (2° S–2° N and 120° E–80° W) from the merged data product^{27,98}.

Timmermann et al., 2018 : El Niño and Southern Oscillation Complexity, Nature (Review)

How to Reconcile Diversity and Complexity of ENSO

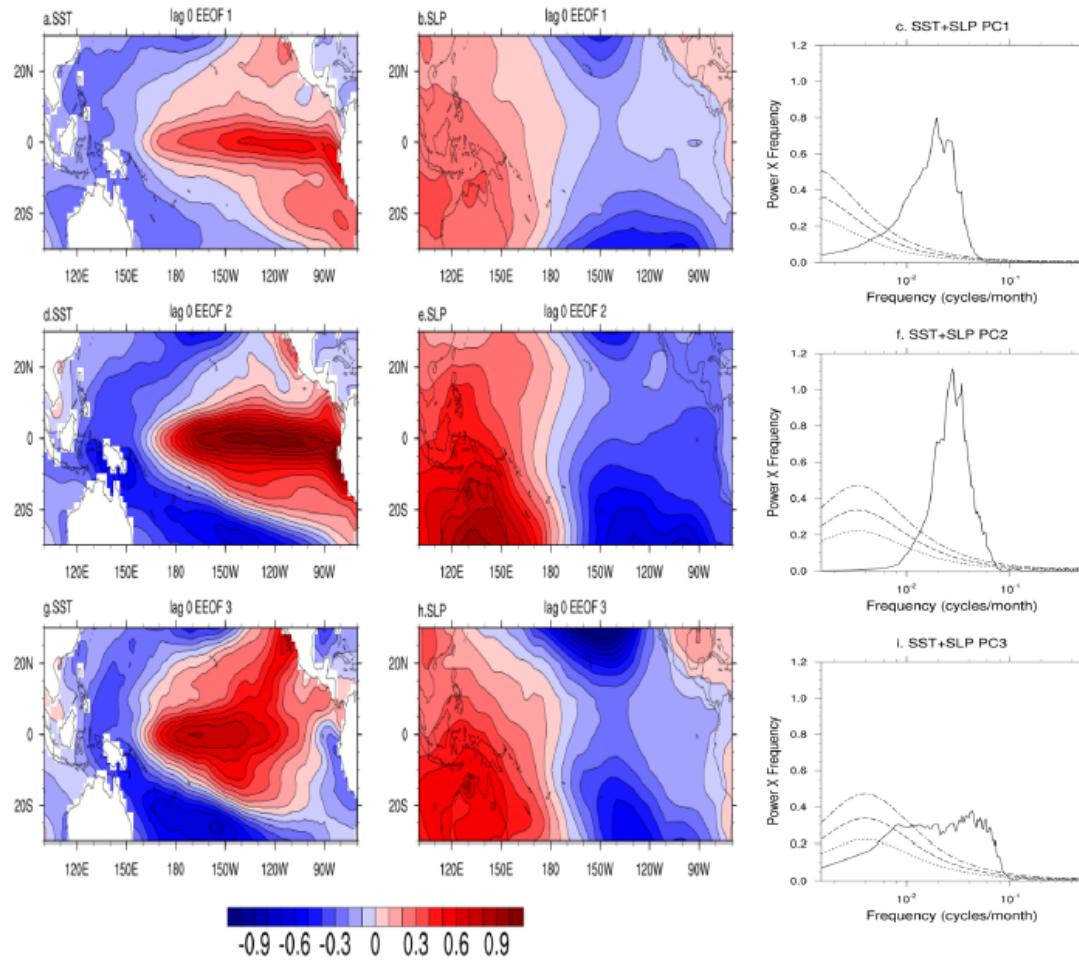


Figure 1. Plot of combined EEOF of SST and SLP based on HADSLP data and ERSST data for the Pacific (30°S–30°N; 100°E–90°W) and with time lag of 18 months used to create the co-variance matrix (see text). (a) EEOF-1 pattern for SST at lag 0, (b) EEOF-1 pattern of SLP at lag 0, (c) Power spectra of principal component of mode 1:PC1; (d-f) same as (a-c) but for mode 2 (EEOF2/PC2); (g-i) same as (a-c) but for mode 3 (EEOF3/PC3).

Chattopadhyay R., S. A. Dixit & B. N. Goswami, 2019: A Modal Rendition of ENSO Diversity, Nature Scientific Reports

Some recent Reviews

Chunzai Wang , Paul C. Fiedler, 2006: ENSO variability and the eastern tropical Pacific: A review, Progress in Oceanography 69 (2006) 239–266

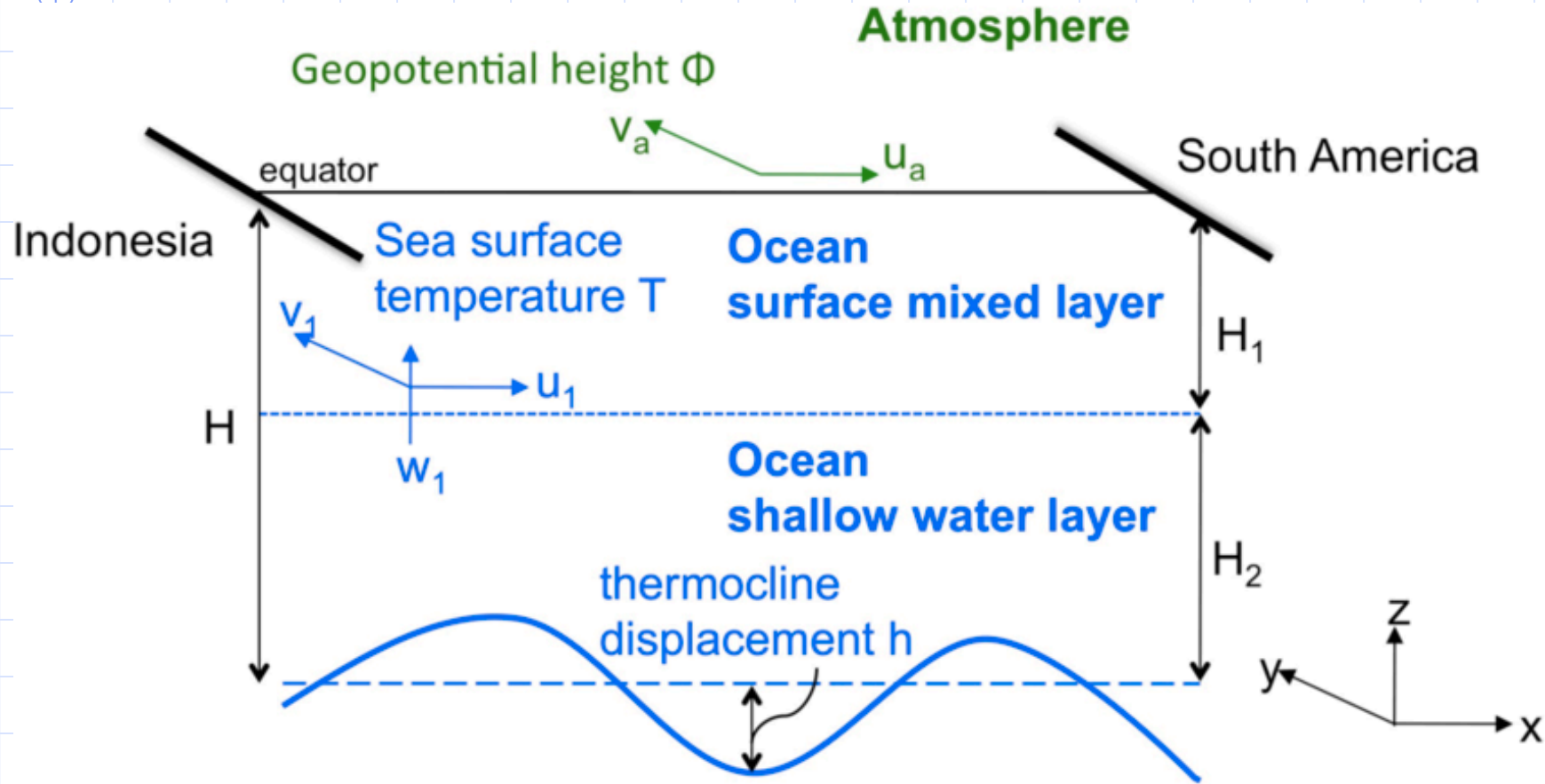
Wang C et al, 2016: El Niño and Southern Oscillation (ENSO), A Review, in Coral Reefs in the Eastern Pacific, P.W. Glimm et al (Eds), Springer

Nan Chen et al, 2019: El Niño and the Southern Oscillation: Theory, in Reference Module in Earth System and Environmental Sciences, Elsevier,

Nan Chen and S. Zebiak, 2019: El Niño and the Southern Oscillation: Observation, in Reference Module in Earth System and Environmental Sciences, Elsevier,

Predictability of ENSO

Used Cane-Zebiak Coupled model to make predictability experiments



Goswami B. N. and J. Shukla, 1991: Predictability of a coupled ocean-atmosphere model, J. Climate, 4, 3-22

Predictability of ENSO

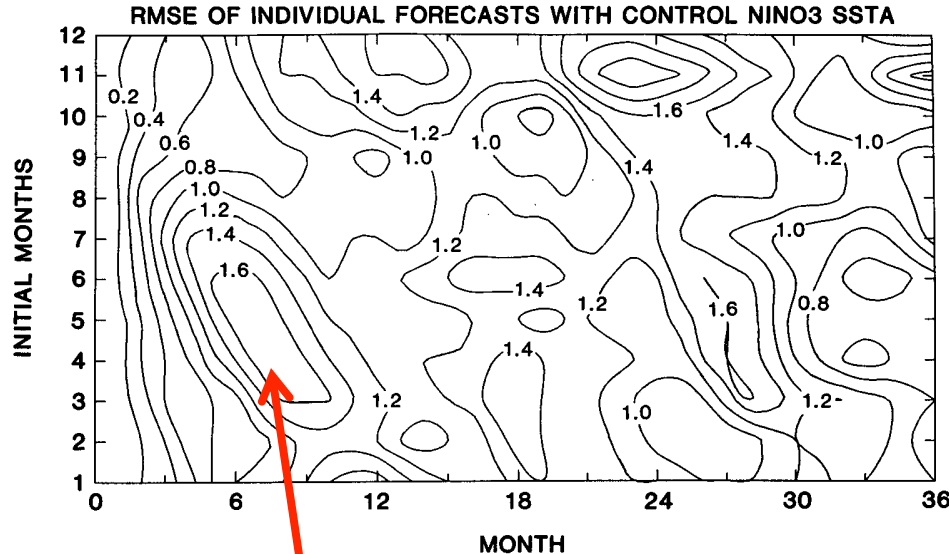


FIG. 7. Dependence of rms ($P - C$) error of individual forecasts on the initial conditions corresponding to different months of the year (1–12 refer to January–December, respectively). Contour interval is 0.2°C .

Spring Predictability barrier

From 181 pairs of identical twin predictability experiments, two time scales of error growth



Doubling time scale, $T_1 \sim 5$ months
Doubling time scale $T_2 \sim 15$ months

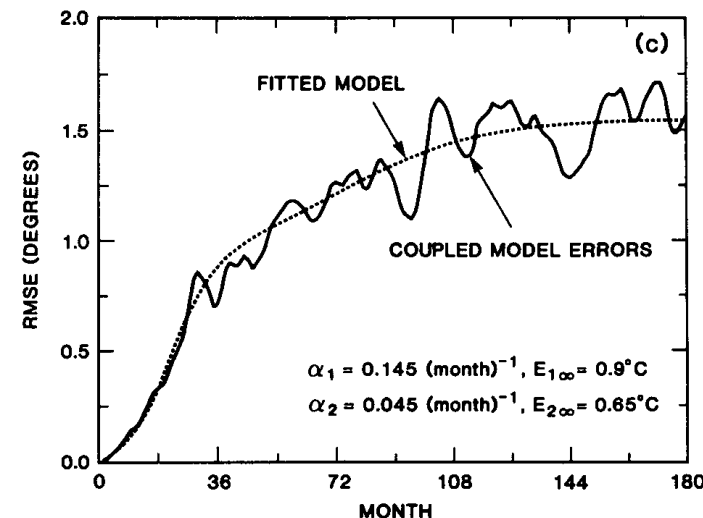
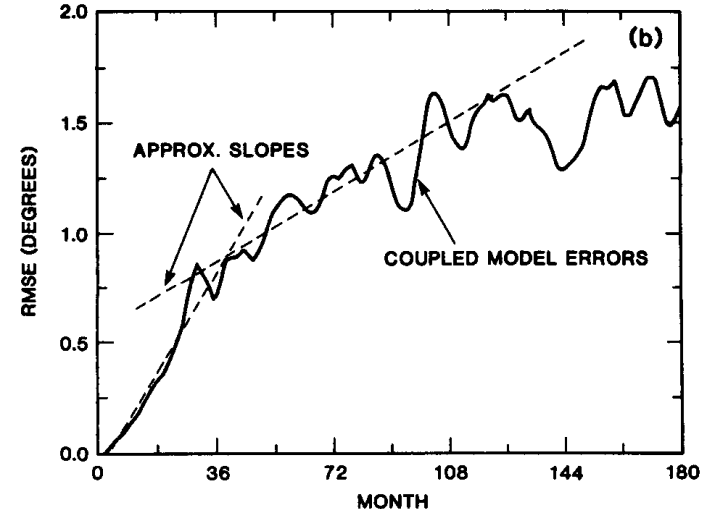


FIG. 10. Empirical model for the growth of small errors. (a) Growth of one-month ($P - C$) errors (solid) and the fitted model (dotted). (b) Same as (a) but rms error from 151 identical twin experiments due to small random initial perturbation on the surface winds. The dashed curves show approximately the two different slopes of the curve. (c) The fitted model for the error curve in (b).



Thank You